



# Upper Airway Radiology

Richard J. Schwab and Andrew Wiemken

Upper airway imaging provides important knowledge about the pathogenesis and treatment of obstructive sleep apnea (OSA). It allows for the characterization of the size of the upper airway, the surrounding pharyngeal soft tissue, and craniofacial structures. Upper airway imaging can be static or dynamic and can be performed during sleep. It can also provide key information about the anatomic changes with CPAP (continuous positive airway pressure), oral appliances, weight loss, and upper airway surgery. Such information can provide insights into the mechanism of action of different treatments for sleep apnea.

## 1 Different Imaging Modalities to Examine the Upper Airway

Many different imaging modalities can evaluate the upper airway lumen, pharyngeal soft tissues, and craniofacial structure. These include the following: (1) cephalometrics can examine a two-dimensional skeleton; (2) nasopharyngoscopy can examine pharyngeal lumen awake and asleep (drug-induced sleep endoscopy); (3) ultrasound can examine pharyngeal anatomy without radiation; (4) PET (positron emission tomography) in conjunction with CT (computed tomography) or MRI (magnetic resonance imaging) can examine tongue metabolic function and upper airway inflammation; (5) CT can examine static and dynamic pharyngeal anatomy; and (6) MRI can examine static (volumes of the upper airway soft tissues including tongue fat), dynamic upper anatomy and state-dependent imaging. In this chapter, we will discuss each of these imaging modalities in more detail and how they provide insights into the diagnosis and management of patients with OSA.

R. J. Schwab (✉) · A. Wiemken  
Department of Medicine, Division of Sleep Medicine, University of Pennsylvania Medical Center, Philadelphia, PA, USA  
e-mail: [rschwab@penndmedicine.upenn.edu](mailto:rschwab@penndmedicine.upenn.edu)

## 2 Insights into the Pathogenesis of OSA with Static Upper Airway Imaging

There are a number of different imaging modalities that have provided important insights into the pathogenesis of OSA. Cephalometrics (Fig. 1) has been utilized in many studies to study static craniofacial anatomy [1, 2]. The lateral cephalogram is a standardized lateral view radiograph of the head and neck that provides information on bony and soft tissue structures. Cephalometric imaging can determine if a patient is retrognathic, but it is only a two-dimensional representation examining anterior-posterior anatomy and does not provide information on lateral structures. CT (Figs. 2, 3, 4, and 5) and MRI (Figs. 6, 7, and 8) scanning provides high resolution 3-D representation of the upper airway lumen, soft tissues, and craniofacial anatomy [3]. MRI in particular has provided novel insights into the pathogenesis of OSA. An MRI study [4] has shown that upper airway volume is smallest in the retropalatal region and smaller in apneics than controls. That study [4] also showed that the volume of the soft tissue structures surrounding the upper airway is enlarged in patients with sleep apnea and that this enlargement is a significant risk factor for sleep apnea. In particular, after covariate adjustments, the volume of the tongue, lateral pharyngeal walls, and total soft tissue was significantly larger in patients with sleep apnea than in normal subjects. These data also demonstrated that the larger the volume of the tongue, lateral pharyngeal walls, and total soft tissue, the greater the risk of developing sleep apnea.

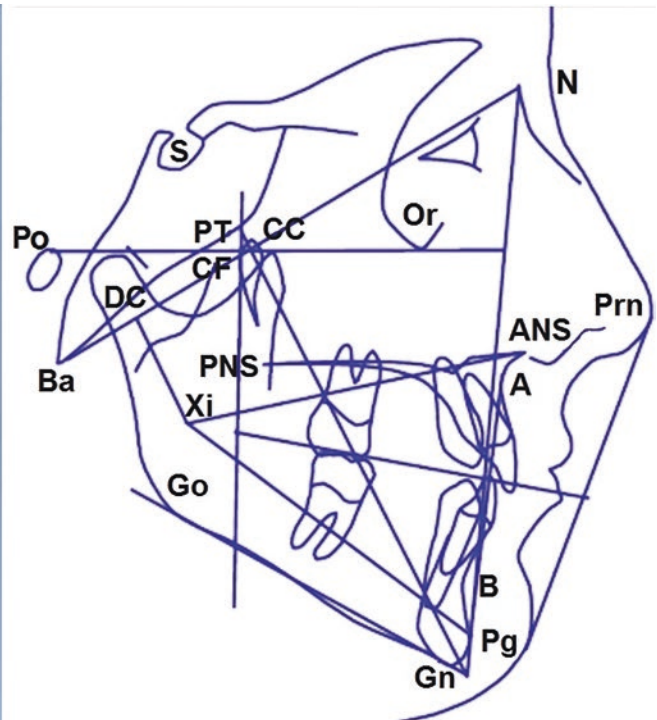
One of the reasons tongue size is greater in patients with sleep apnea is related to increased tongue fat (Figs. 9, 10, and 11) and may explain the relationship between obesity and sleep apnea. An MRI study [5] using Dixon imaging (a method to specifically image fat) to examine tongue fat demonstrated: (1) apneics have greater tongue volumes and more fat within the tongue compared to control subjects, after adjustments for age, BMI, gender, and race; (2) in both apneics and controls, more fat was present in the tongue than in a

control upper airway muscle (masseter); (3) tongue fat percentage was greater in the retroglossal region compared to the retropalatal region; and (4) tongue fat volume correlated with BMI (body mass index) and AHI (apnea–hypopnea index).

MRI can also examine craniofacial dimensions (Figs. 12, 13, and 14). In a case-control study [6] using three-dimensional magnetic resonance imaging cephalometry in 55 apneics and 55 controls matched for age, sex, and race, the following was found: (1) a 1-SD increase in mandibular length and depth were associated with decreased risk of sleep apnea in men but not in women and (2) increases in hyoid-to-nasion and supramentale-to-hyoid distances were associated with increased risk of OSA in both men and women. In this study [6], a smaller and shallower mandible was an independent risk factor for OSA in males, but not females, and the size of the mandible (length and depth) was a much more important risk factor for OSA than maxillary

measures or angular measurements [SNA (angle between sella, nasion, and subspinale point A) and SNB (angle between sella, nasion, and supramentale point B)].

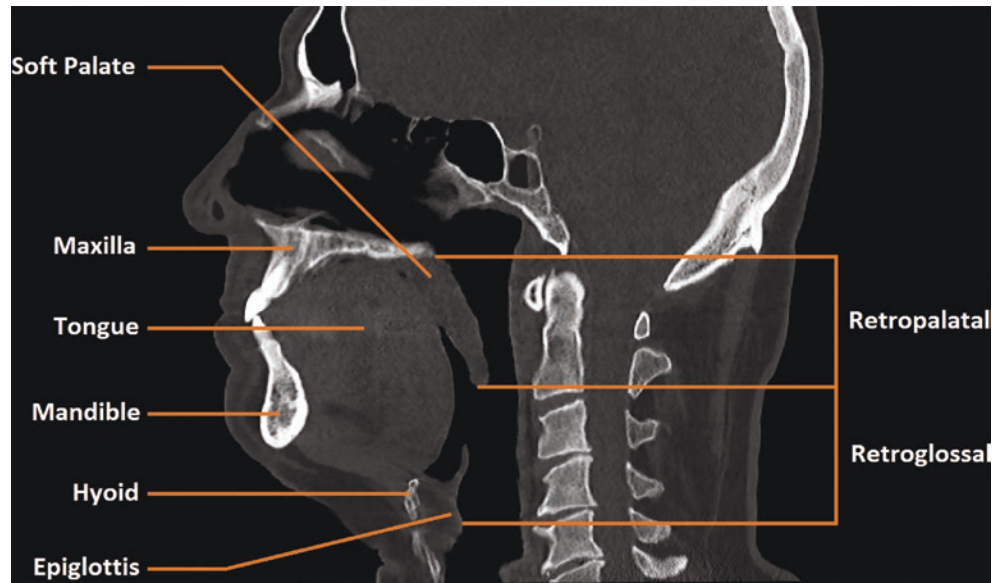
Ultrasound has also been shown to have the capability of measuring tongue size (Fig. 15) and tongue fat (Fig. 16). Studies have used submental ultrasound to characterize the tongue in OSA, showing that increased tongue width and tongue thickness are associated with severe OSA [7–10]. Tongue fat [11] can also be determined with ultrasound. In this study, echo intensity of the tongue base strongly correlated to the fat percentage for both the posterior tongue and the entire tongue measured with MRI. Larger tongue fat percentages and higher echo intensity were associated with a higher apnea–hypopnea index, after adjustments for age, body mass index, sex, and race. Thus, ultrasound could be used as an alternative method to quantify tongue fat since this modality is faster, cheaper, and more easily accessible than MRI.



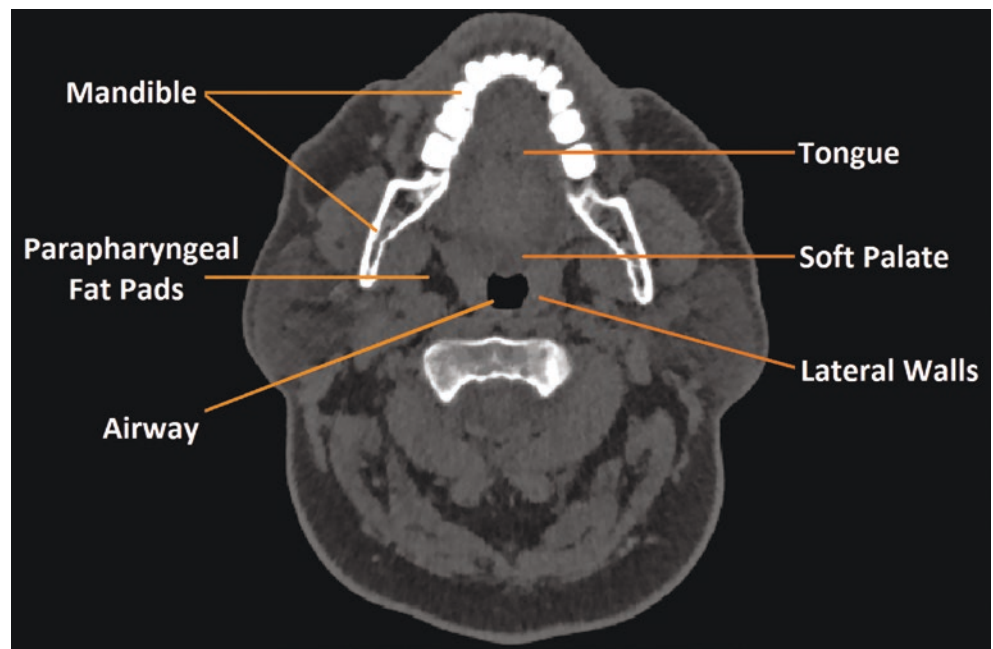
**Fig. 1** Cephalometric X-ray. The left panel is the cephalometric X-ray and on the right panel are the key craniofacial measurements that can be obtained from this radiograph. Cephalometric landmarks: (1) A—A point/subspinale, most concave point of the anterior maxilla. (2) B—B point/supramentale, most concave point of the anterior mandibular symphysis. (3) Pr—Porion, superior point of the external auditory meatus. (4) Ba—Basion, anterior point of foramen magnum. (5) N—Nasion, most concave anterior point of the nasal bridge. (6) DC—Condyle at the intersection with basion-nasion plane. (7) Go—gonion, most convex posterior point of the mandibular body at corpus-ramus

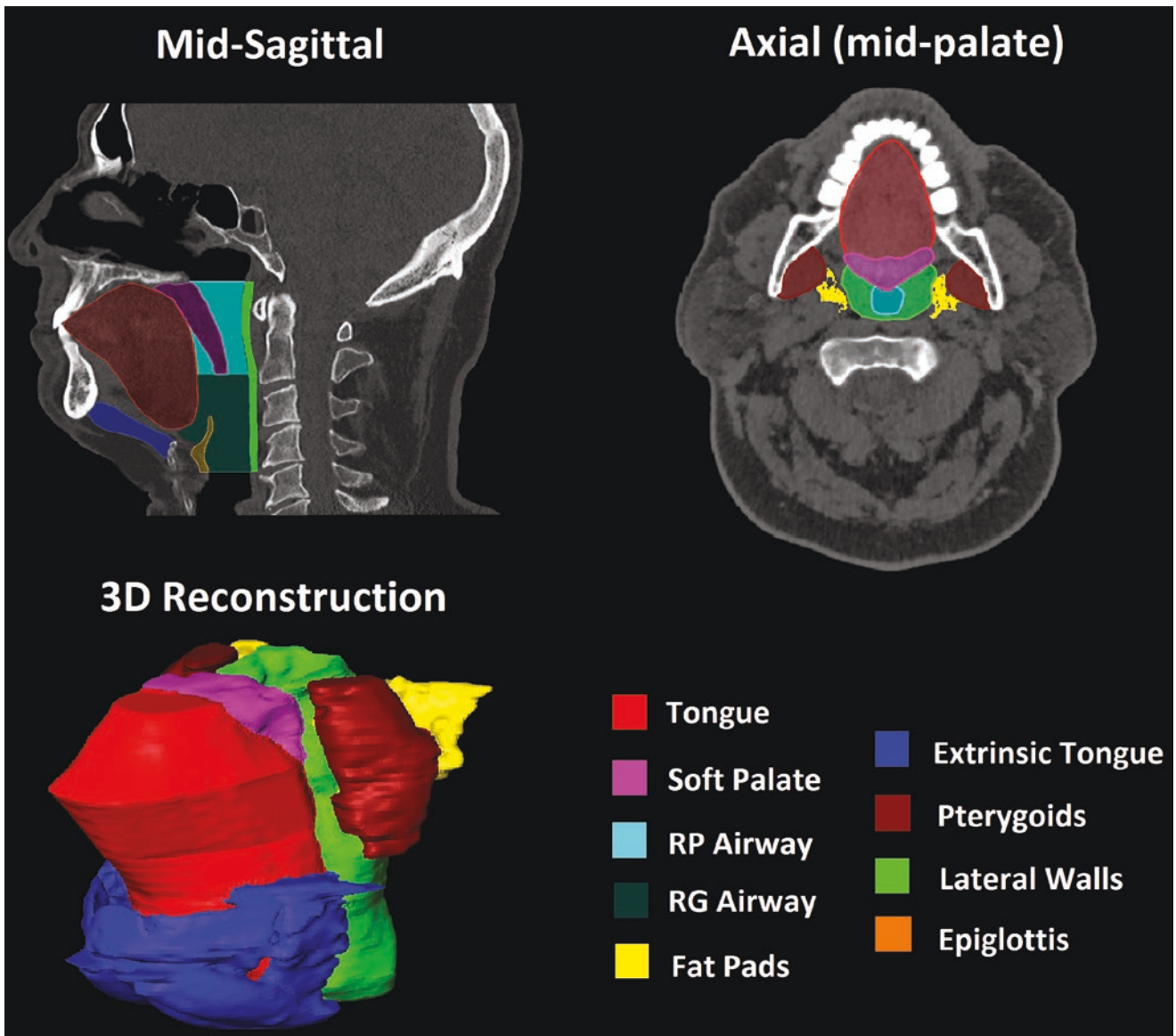
junction. (8) Xi—Xi point, geometric center of mandibular ramus. (9) ANS—Anterior nasal spine. (10) PNS—Posterior nasal spine. (11) PT—PT point, intersection of pterygomaxillary fissure and foramen rotundum. (12) CF—Center of face, intersection of pterygoid with Frankford plane. (13) S—Sella, the centroid of sella turcica @ seat of the pituitary gland. (14) CC—Center of cranium. (16) Or—Orbitale, most inferior point of orbit margin. (17) Prn—Pronasale, soft tissue tip of the nose. (18) Pg—Pogonion, most convex anterior point of the mandibular symphysis. (19) Gn—Gnathion, most anterior-inferior point of the mandibular symphysis

**Fig. 2** CT mid-sagittal image of the upper airway. Highlighting the airway regions (retropalatal—from the level of hard palate to caudal margin of soft palate; and retroglossal—from caudal margin of soft palate to base of tongue) and important upper airway soft tissues (tongue, soft palate, epiglottis) and craniofacial (maxilla, mandible, hyoid) structures



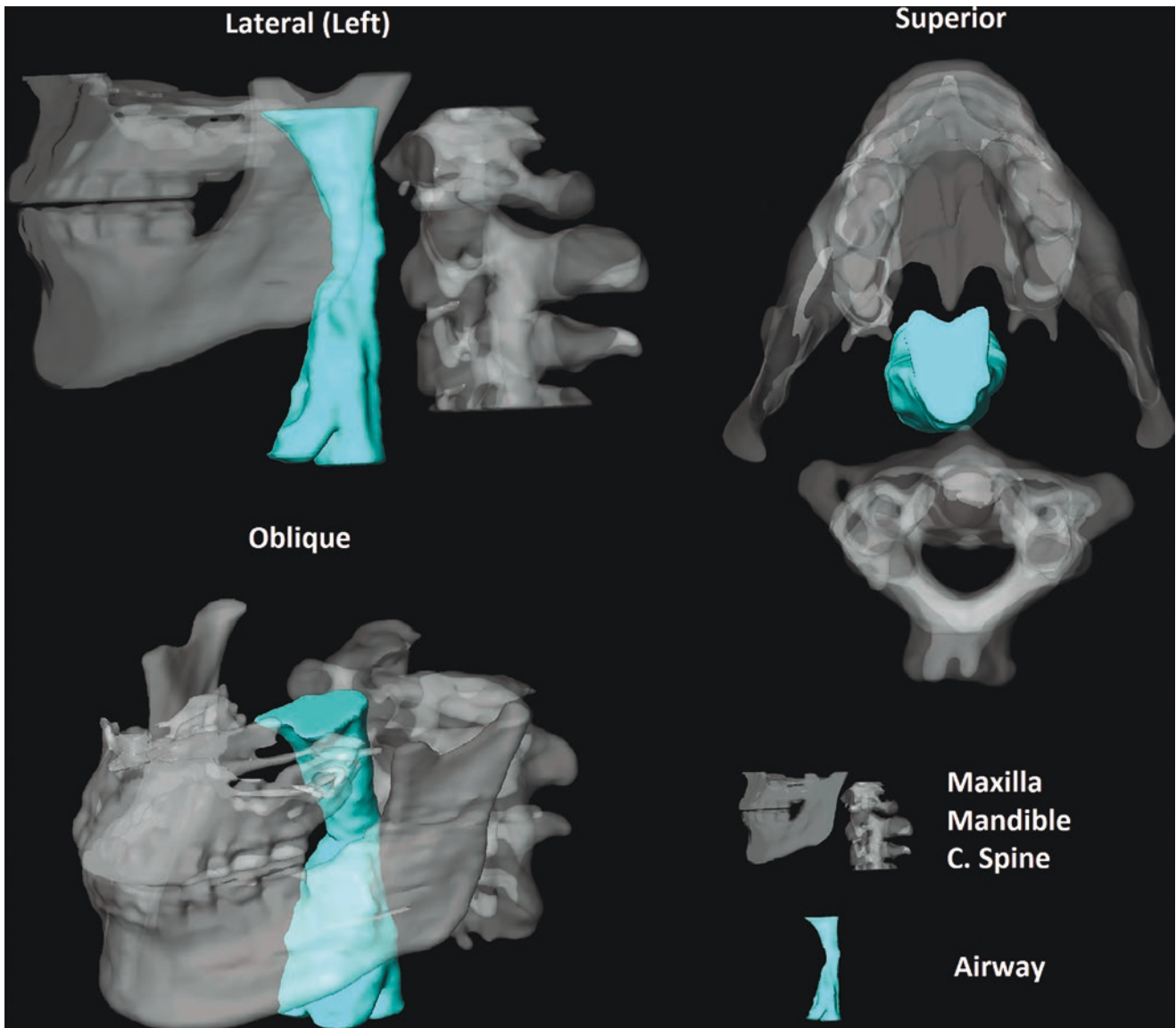
**Fig. 3** CT axial (mid-palate) image of the upper airway. Highlighting the airway and important upper airway soft tissues (tongue, soft palate, lateral pharyngeal walls, parapharyngeal fat pads) and craniofacial (mandible) structures





**Fig. 4** Three-dimensional CT reconstructions of the upper airway. Segmentations of the upper airway (RP {retropalatal} teal, RG {retro-glossal dark green}) and key upper airway soft tissue structures (red = tongue, purple = soft palate, yellow = fat pads, blue = extrinsic

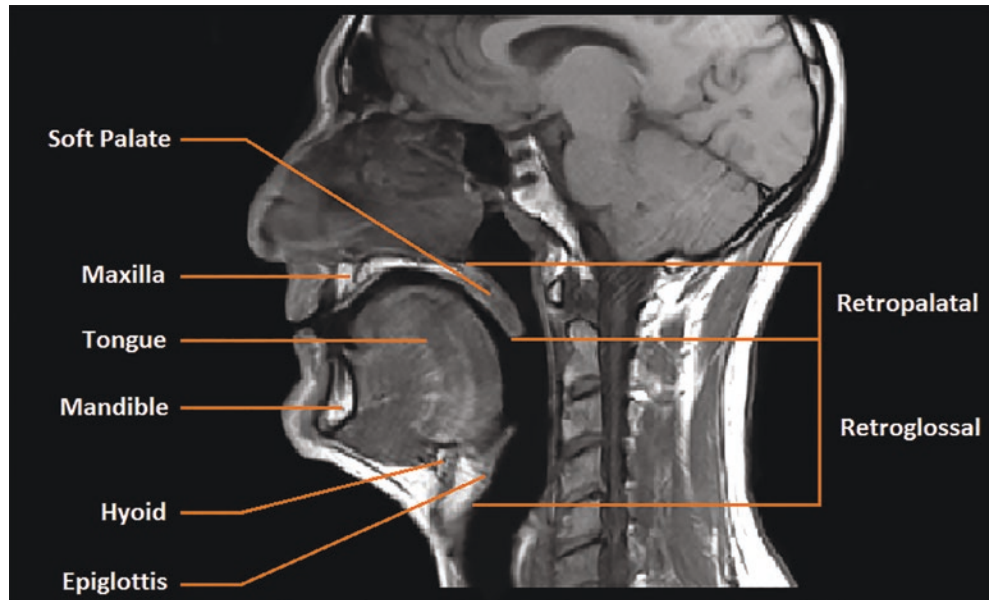
tongue muscles, brown = pterygoids, green = lateral walls, orange = epiglottis on axial (mid-palate) and mid-sagittal views) with a 3D reconstruction showing all the structures together



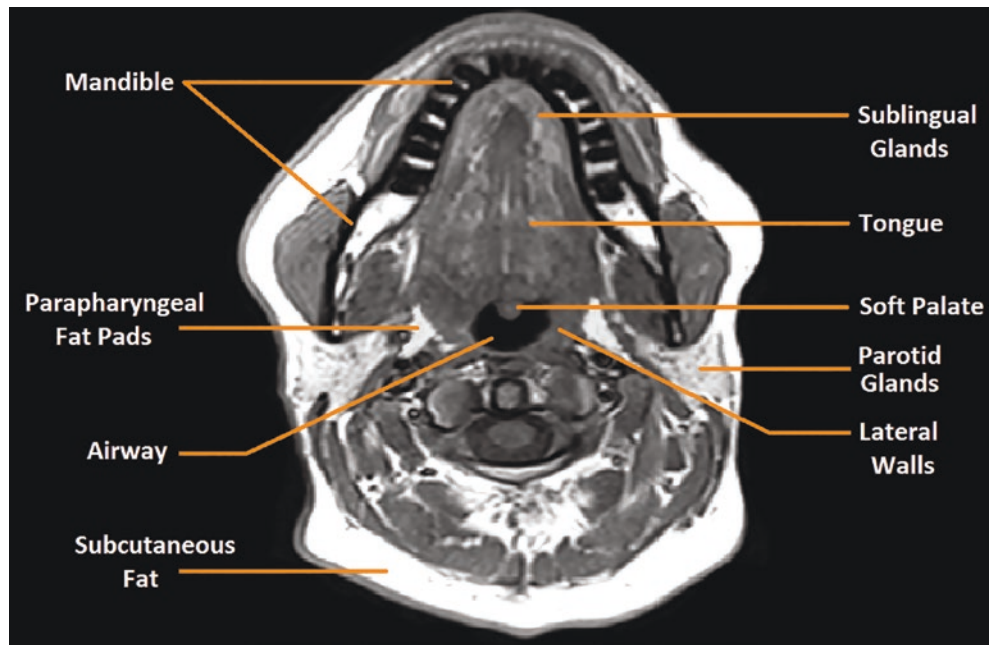
**Fig. 5** Three-dimensional CT bony reconstructions of the upper airway. 3D reconstructions of the maxilla (gray), mandible (gray), cervical (C), spine (gray), and airway (blue) in lateral, superior, and oblique

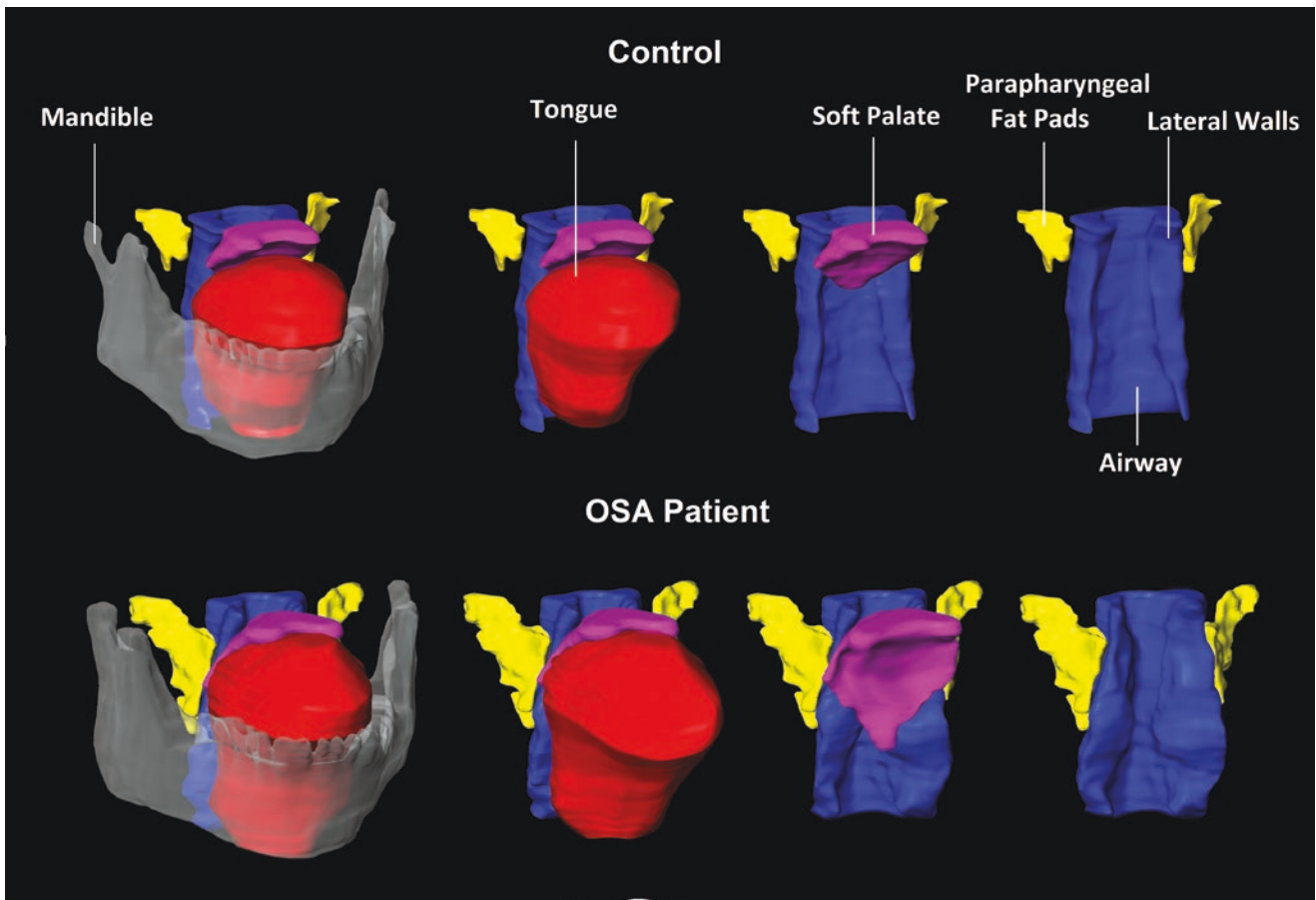
views using CT images of the upper airway. CT scanning is especially good for bony reconstructions of the pharynx

**Fig. 6** MRI mid-sagittal image of the upper airway. Highlighting the airway regions (retropalatal—from the level of hard palate to caudal margin of soft palate; and retroglossal—from caudal margin of soft palate to base of tongue) and important upper airway soft tissues (tongue, soft palate, epiglottis) and craniofacial (maxilla, mandible, hyoid) structures



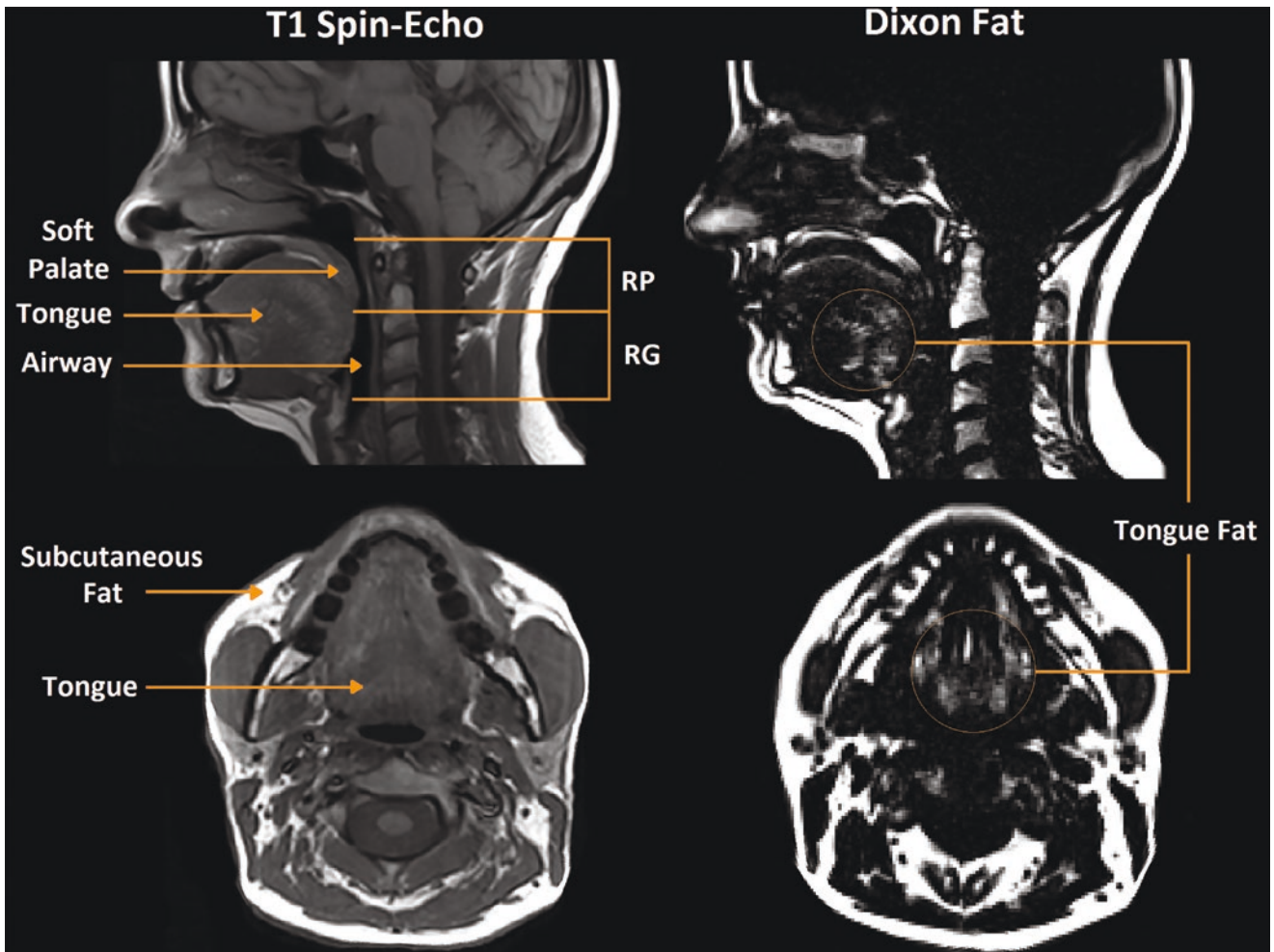
**Fig. 7** MRI axial (mid-palate) image of the upper airway. Highlighting the airway and important upper airway soft tissues (tongue, soft palate, lateral pharyngeal walls, parapharyngeal fat pads, parotid glands, sublingual glands, subcutaneous fat) and craniofacial (mandible) structures





**Fig. 8** Three-dimensional MRI reconstructions of the upper airway in a weight matched control subject and a patient with sleep apnea. 3D reconstructions of the key upper airway soft tissue (red = tongue, purple = soft palate, yellow = fat pads, blue = lateral walls) and cra-

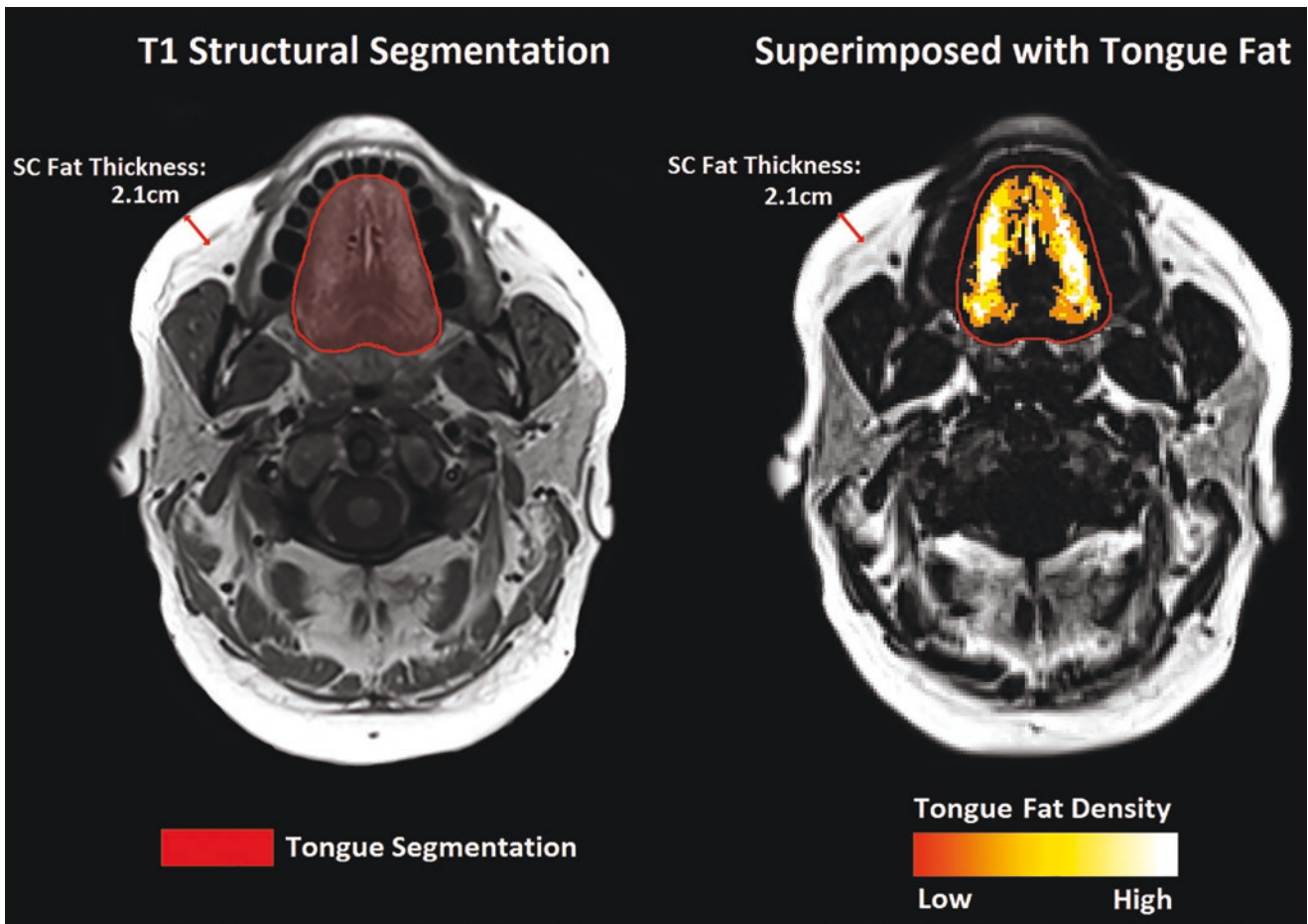
niofacial (gray = mandible) structures. Note that the size of the tongue, soft palate, fat pads, and lateral walls are larger in the patient with sleep apnea. The airway is smaller in the patient with sleep apnea



**Fig. 9** Measurement of tongue fat. Comparison of tongue fat using standard T1-weighted spin echo MR imaging vs. fat-weighted Dixon MR imaging in a patient with sleep apnea. Airway regions (retropalatal and retroglottal) and surrounding soft tissue structures (soft palate,

tongue, tongue fat) are denoted with arrows. Both sagittal images are mid-sagittal and axial images are shown at the same level of the (mid) tongue. Note that fat deposits in the tongue are more easily visualized using the Dixon MR imaging sequence than with the spin echo sequence

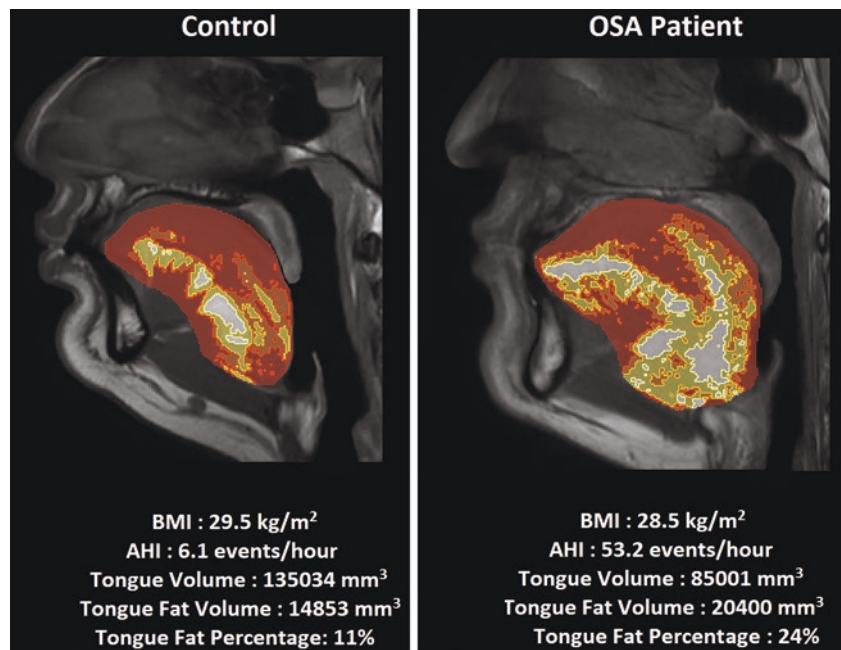


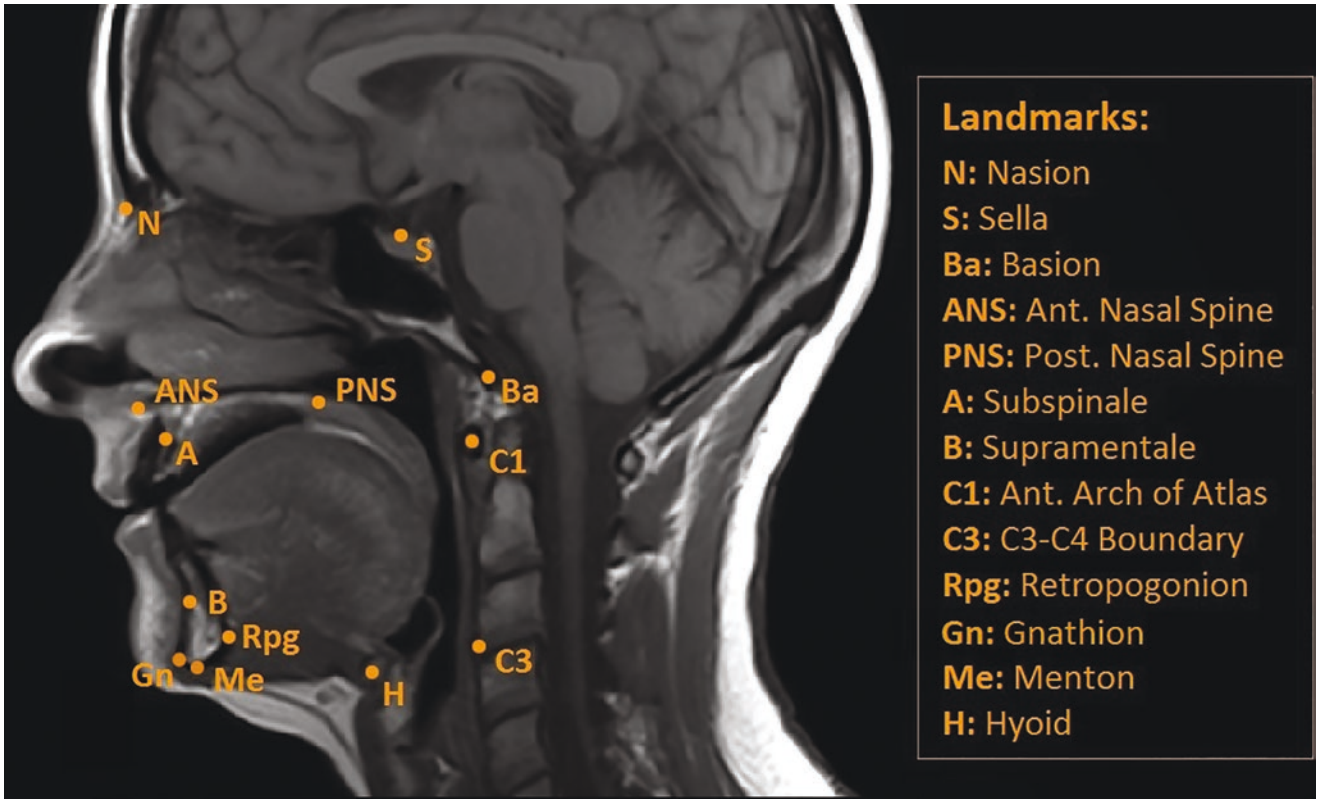


**Fig. 10** Measurement of tongue fat - segmentation. Axial standard T1-weight spin echo and fat-weighted Dixon MR images of the upper airway. Segmentation of the apneic tongue using standard T1-weighted spin echo MR image with superimposed segmentation on correspond-

ing anatomic level of a Dixon image. Note that there are comparable thicknesses of subcutaneous fat on each image indicating appropriate scaling

**Fig. 11** Tongue fat—volumetric reconstruction. Representative three-dimensional volumetric reconstructions of tongue (red) and fat within tongue (yellow) from a series of 3-mm contiguous axial MR images superimposed on midsagittal images in BMI-matched control subject (left) and patient with OSA (right). Note the apneic tongue in the patient with sleep apnea is much larger and there is increased tongue fat deposition throughout the apneic tongue

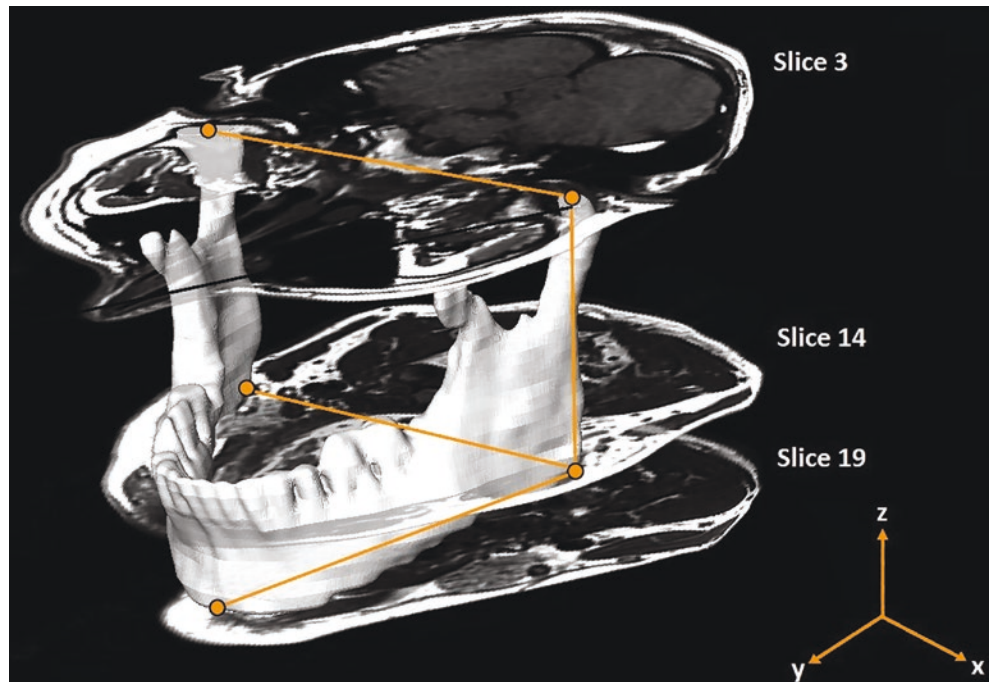




**Fig. 12** MR cephalometry. Spin echo MRI can be used to obtain cephalometric points and measurements. Rpg—Retropogonion, most convex posterior point of the mandibular symphysis. H—Hyoid, the centroid of hyoid at the midline. Me—Menton, most inferior point of

the mandibular symphysis. C1—Anterior arch of atlas. “C3”—C3–C4 boundary, most anterior point of spine between C3 and C4. See Fig. 1 for an explanation of other measures

**Fig. 13** MR cephalometry—mandibular measurements. Three-dimensional reconstruction of the mandible with measurements of mandibular length and width. Linear distances are computed mathematically from Cartesian coordinates (z-axis determined by slice number and thickness)



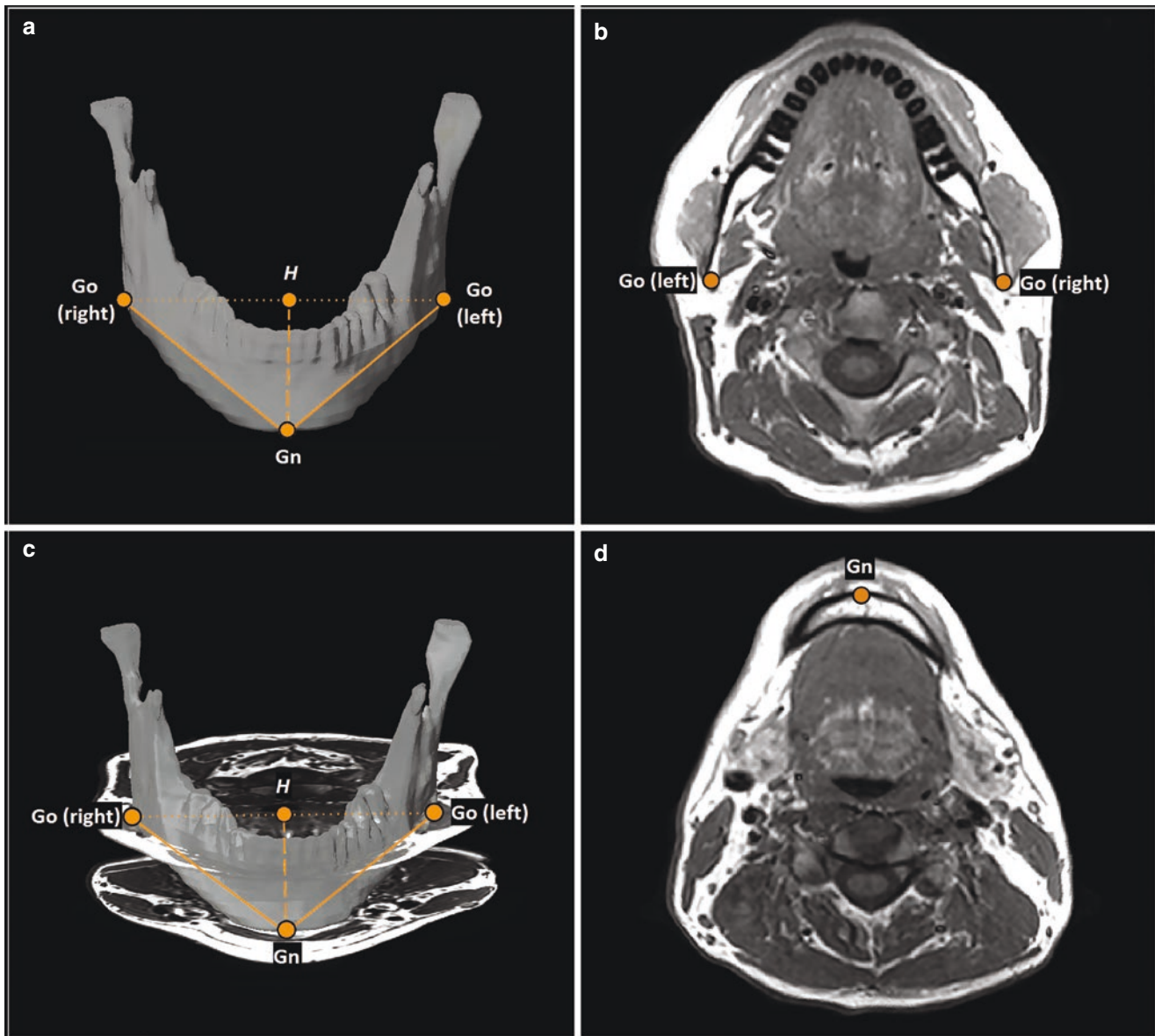


**Fig. 14** MR cephalometry—mandibular measurements. Three-dimensional reconstruction of the mandible (**a**, **c**—shows the actual MRI axial slices in addition to the reconstruction) with craniofacial points and distance measurements. Craniofacial points include: gnathion (Gn), the most anterior–inferior point of the mandible; gonion (Go), the left and right Go are the most posterior and inferior points of the mandible. The distances measured: mandibular body length (—),

the distance from Gn to the left or right Go; mandibular width (---), the two-dimensional measurement of the width of the lower portion of the mandible (the distance between the left and the right Go); mandibular depth (---), the distance from Gn to H, where H is the midpoint between the left and the right Go. (**b**) The axial MR slice containing the left and right Go. (**d**) The axial MRI slice containing the Gn

**Fig. 15** Tongue ultrasound (US). Placement of the probe and relevant upper airway anatomy (tongue, mylohyoid, dermis) visualized with submental US

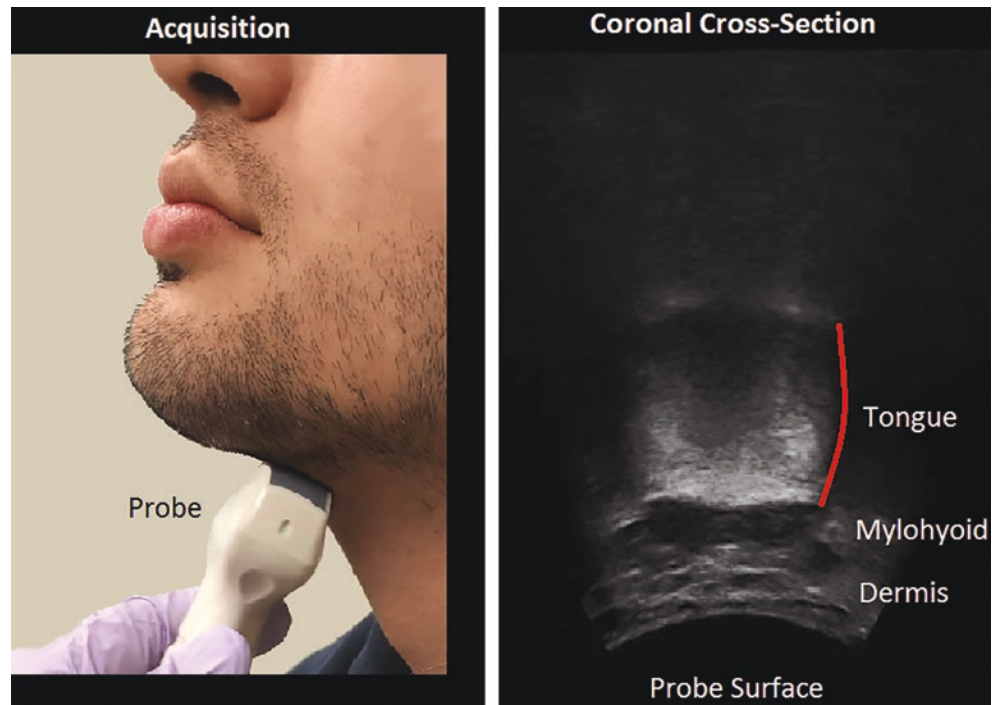
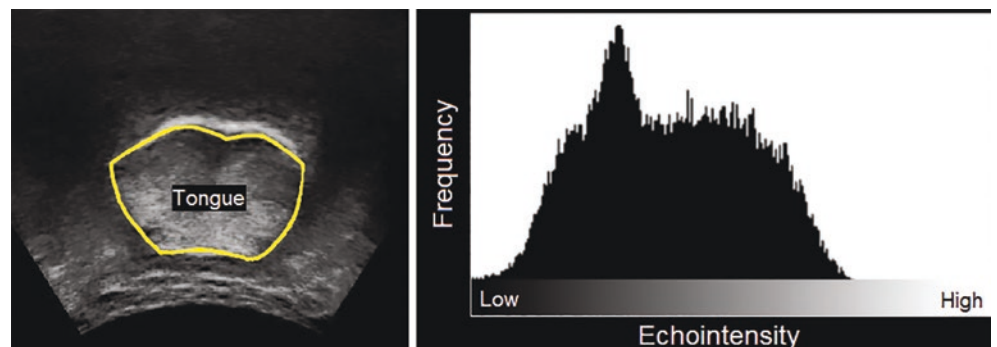


**Fig. 16** Tongue echo intensity to determine tongue fat. Echo intensity calculation. A line (yellow) was drawn bordering the edges of the tongue and the mean gray scale intensity within the tongue was recorded. Next, a comparison of ultrasound echo intensity was compared to MRI as a metric for tongue fat



### 3 Insights into the Pathogenesis of OSA with Dynamic Upper Airway Imaging

Dynamic upper airway imaging can be performed with cine CT (Fig. 17) or cine MRI (Fig. 18, 19, and 20). Unlike static imaging, dynamic magnetic resonance imaging provides the capability of studying upper airway respiratory-related changes. A study [12] with dynamic MRI has shown: (1) airway area in the retropalatal region was significantly smaller in obese subjects with apnea compared with obese control subjects, controlling for sex, age, BMI, and race; (2) airway narrowing in apneics was observed in both lateral and AP dimensions in the retropalatal region; and (3) there were strong correlations between AHI (apnea–hypopnea index) and many of the dynamic airway measures in both retropalatal and retroglottal regions.

The primary finding of this study [12] was that the retropalatal and not the retroglottal region of the upper airway

was significantly narrower in obese subjects with apnea than in obese control subjects during respiration. These findings provide further evidence that retropalatal airway narrowing rather than retroglottal airway narrowing plays an important role in the pathogenesis of obstructive sleep apnea in obese subjects.

Another modality to examine dynamic changes to the pharyngeal lumen is with a nasal endoscope and drug-induced sleep endoscopy (DISE). DISE is typically used by otorhinolaryngologists to determine the site of airway collapse before undergoing upper airway surgery and it is used before hypoglossal nerve stimulation to ensure the patient does not have concentric collapse (a contraindication to hypoglossal nerve stimulation). DISE is typically scored [13] via a VOTE (velum, oropharynx, tongue base, and epiglottis) classification but the airway changes can be quantified (Figs. 21 and 22) [14].

**Fig. 17** Cine CT changes to the upper airway during respiration. Respiratory-related changes to airway cross-sectional area at the retropalatal region. Airway caliber stays relatively constant during inspiration increases in early expiration and then decreases toward the end of expiration. Airway caliber primarily increases in the lateral dimension as compared to the anterior-posterior dimension

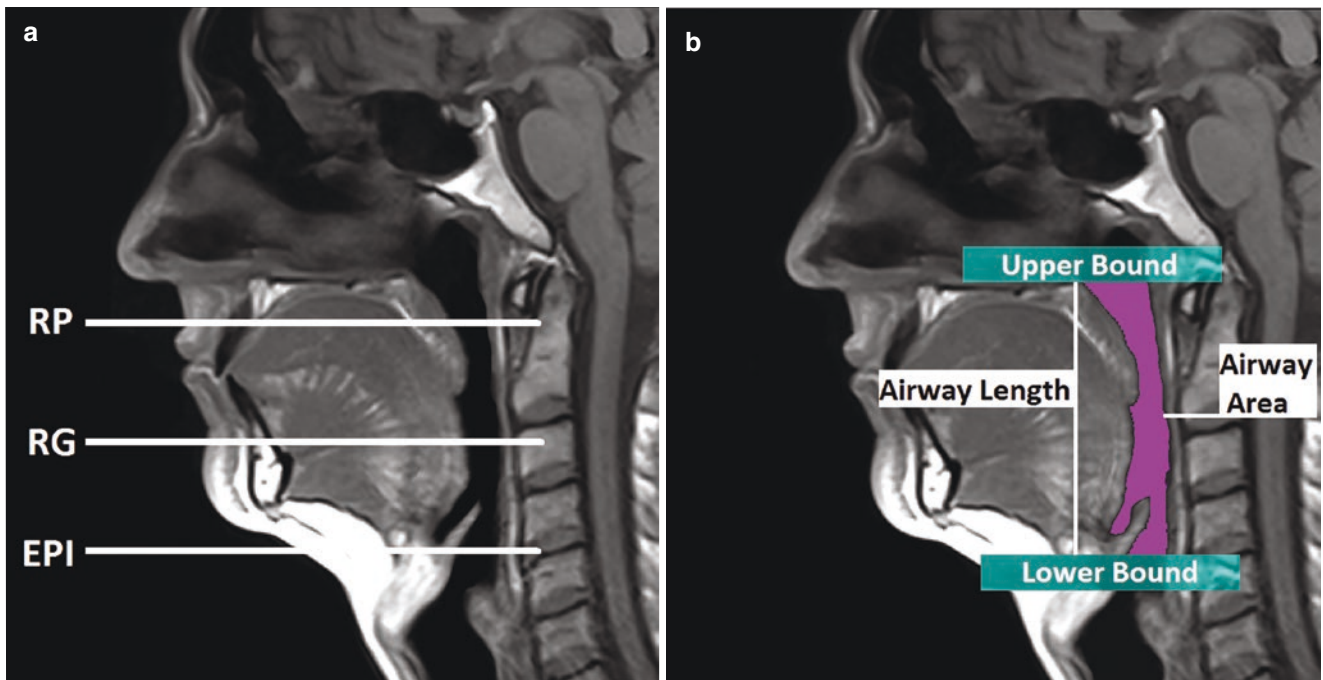
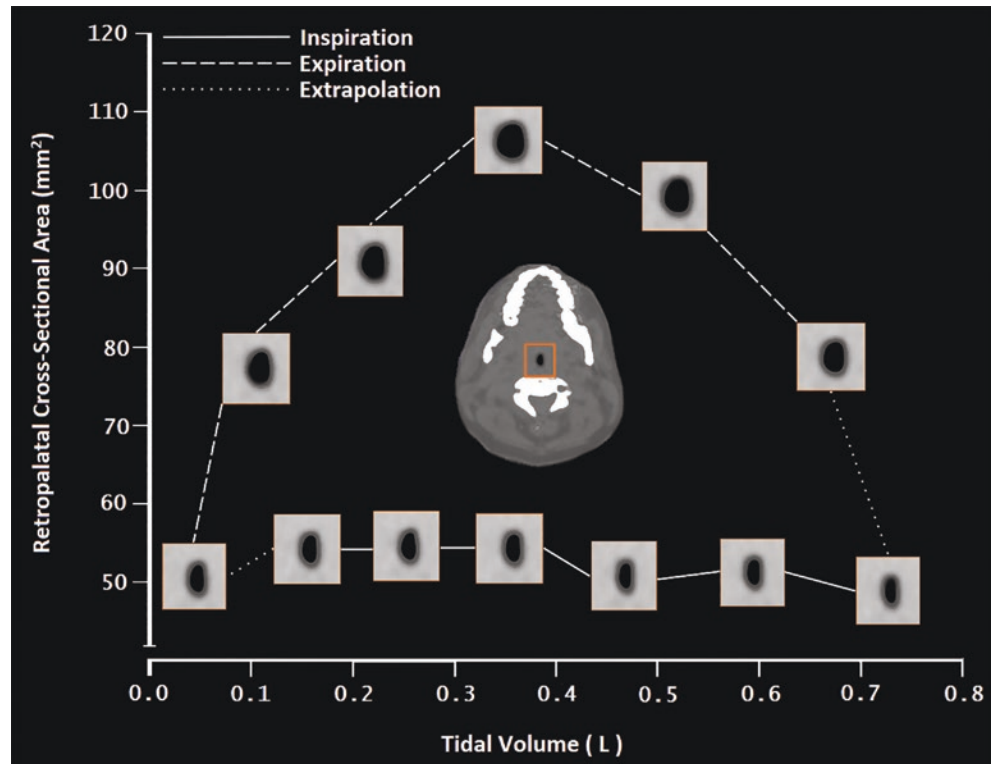


**Fig. 18** Location of dynamic upper airway MR imaging during wakefulness. (a) Mid-sagittal image showing the location of the axial dynamic images (RP {retropalatal}, RG {retroglottal}, and Epi {epiglottal}). (b) Mid-sagittal image showing the upper boundary set

through the top of the hard palate and lower boundary through the bottom of C4; the airway (purple) between these two boundaries represents the mid-sagittal airway area and the perpendicular distance between the two boundaries is the length of the airway

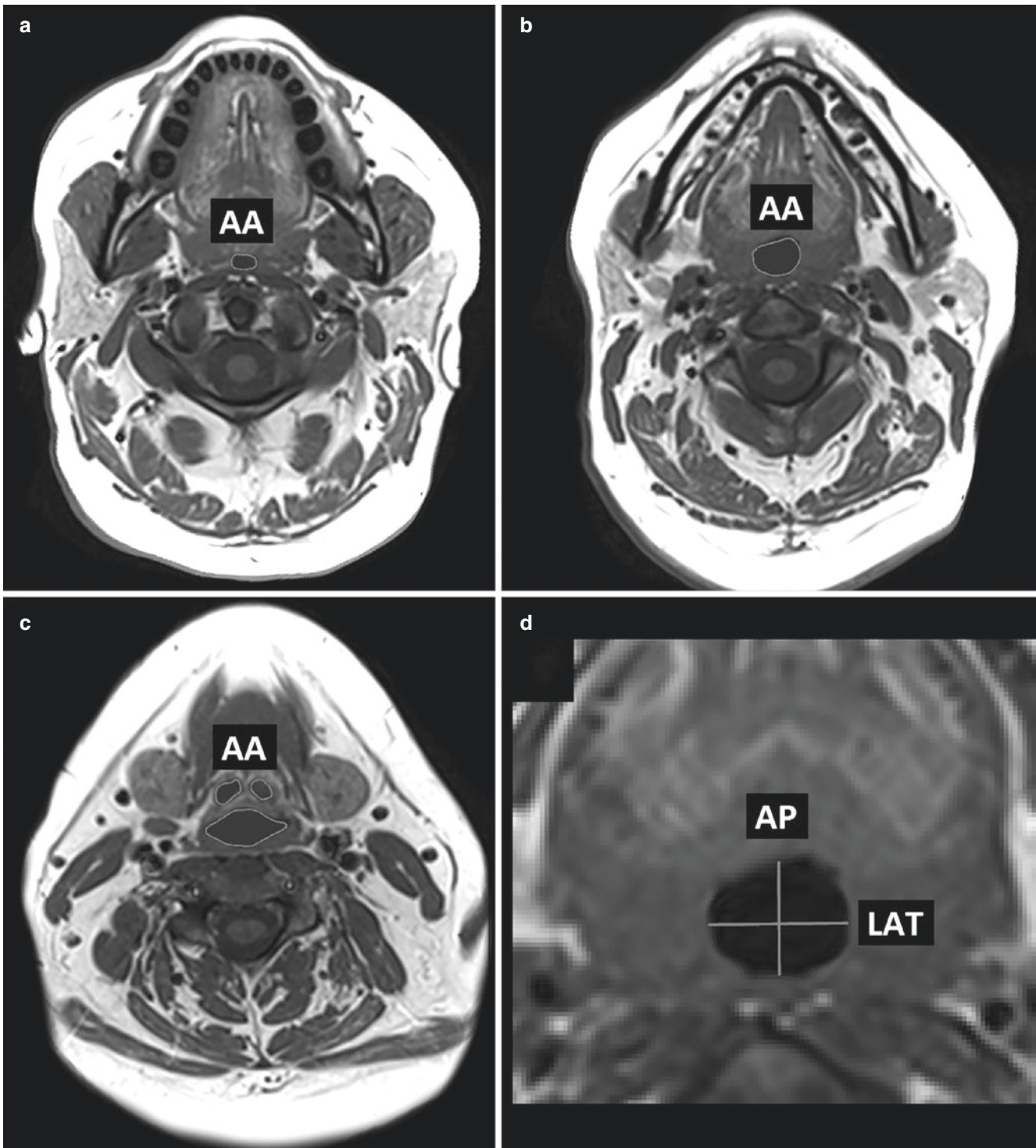


**Fig. 19** Dynamic axial upper airway MR imaging during wakefulness. (a–d) Examples of images in the three axial regions: retropalatal (a) retroglossal (b), and epiglottal (c). (d) shows the method used to mea-

sure airway lateral and anteroposterior dimensions. The lateral (LAT) and anteroposterior dimensions (AP) are measured in the three axial regions. AA airway area

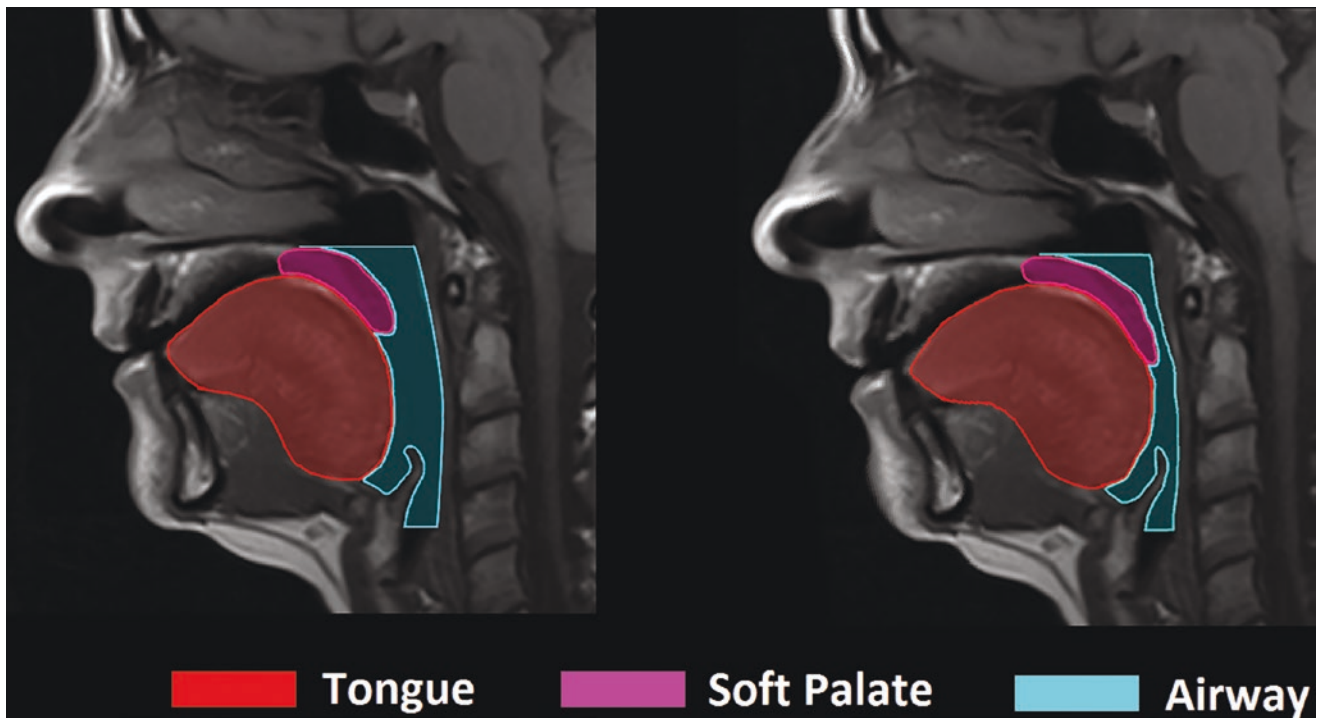


**Fig. 20** Dynamic midsagittal upper airway MR imaging during wakefulness. Midsagittal images were obtained at two different time points during respiration. Airway narrowing is noted in the retropalatal and retroglottal regions during respiration

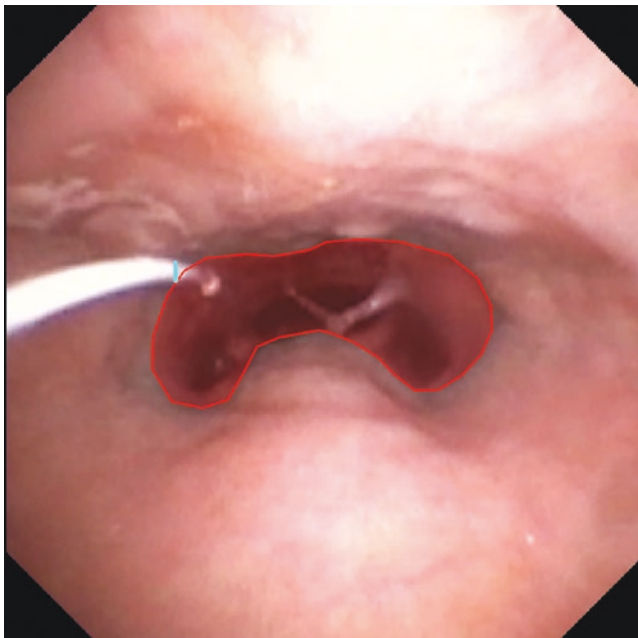


**Fig. 21** Airway lumen in the retropalatal region during DISE. This is an image in the retropalatal region during drug-induced sleep endoscopy (DISE). The airway area is outlined in red. A catheter with a known dimension (blue line) is on the wall of the airway which provides a ruler to quantify airway caliber

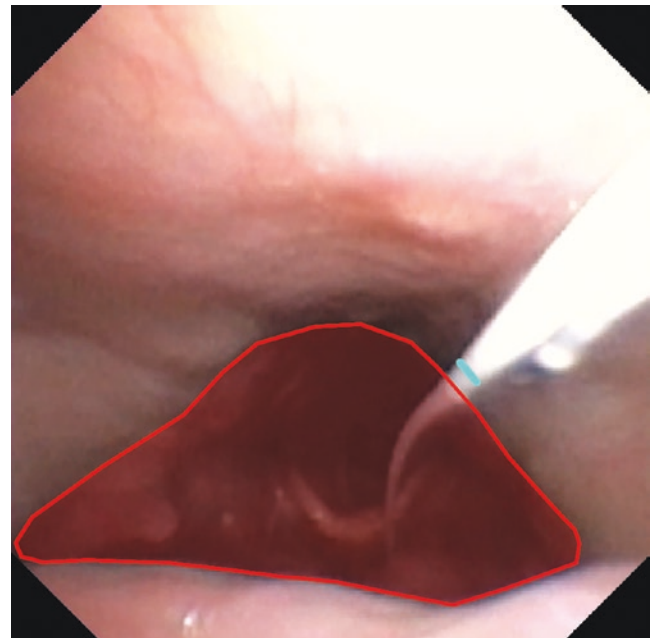


**Fig. 22** Airway lumen in the retroglottal region during DISE. This is an image in the retroglottal region during drug-induced sleep endoscopy (DISE). The airway area is outlined in red. A catheter with a known dimension (blue line) is on the wall of the airway which provides a ruler to quantify airway caliber

#### 4 Insights into the Metabolic Function in OSA Patients with PET Imaging

PET with or without CT or MRI scanning (Figs. 23 and 24) has been utilized to examine metabolic uptake of the tongue. In one study [15] using [18F]-2-fluoro-2-deoxy-D-glucose (FDG) positron emission tomography imaging, there was significantly reduced glucose uptake in the genioglossus (primary dilator muscle of the upper airway) of patients with sleep apnea in comparison with obese normal subjects. Specifically, after adjusting for confounders including age, BMI, sex, and race: (1) FDG uptake was reduced in the genioglossus of patients with OSA compared with control subjects; (2) the results remained unchanged after adjusting for tongue fat; and (3) there were no differences in FDG uptake in other upper airway muscles (masseter, pterygoid)

between patients with sleep apnea and control subjects. These data indicate that there are selective alterations in glucose metabolism within the primary soft tissue structures of the upper airway in patients with OSA. These alterations may be the result of repeated apneas and could directly contribute to OSA. PET imaging offers a new paradigm for understanding the muscle properties of the upper airway soft tissue structures.

PET MRI has also been utilized to examine inflammation in the mucosa of the upper airway [16]. Repetitive upper airway collapse during apneic events can result in upper airway inflammation. This inflammation measured by PET/MRI has been shown [17] to be reduced with CPAP therapy in adults with OSA. Adult OSA patients underwent [18F]-fluoro-2-deoxy-D-glucose (FDG)-PET/MRI of the neck before and after 3 months of using CPAP [17].

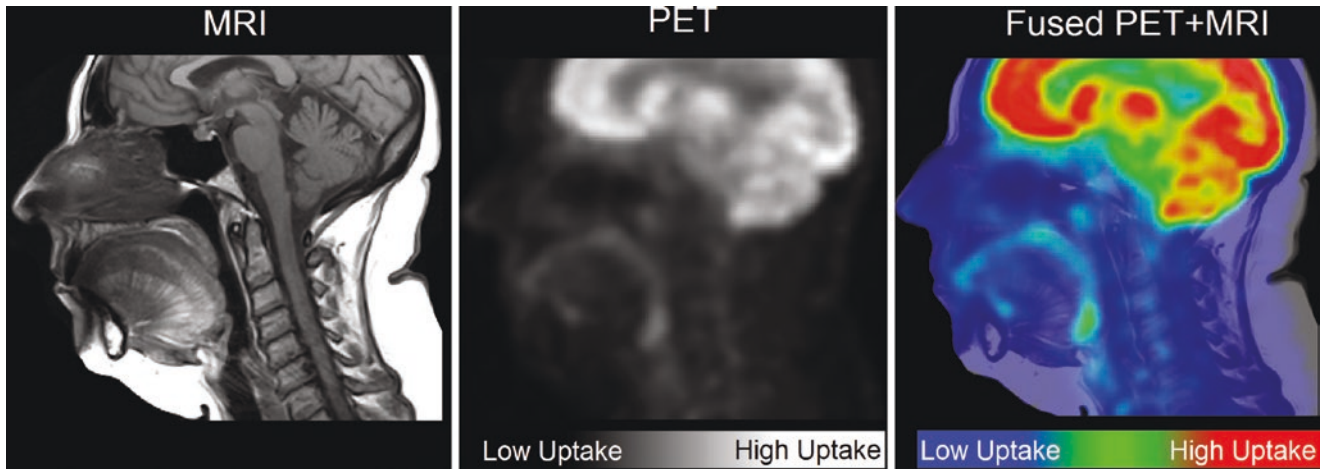


**Fig. 23** PET imaging of the upper airway. Representative magnetic resonance imaging (MRI), positron emission tomography (PET), and fused PET-MRI of the upper airway in a patient with sleep apnea. Color

bars below the PET and fused MRI-PET image indicate high uptake (red) and low uptake (blue)



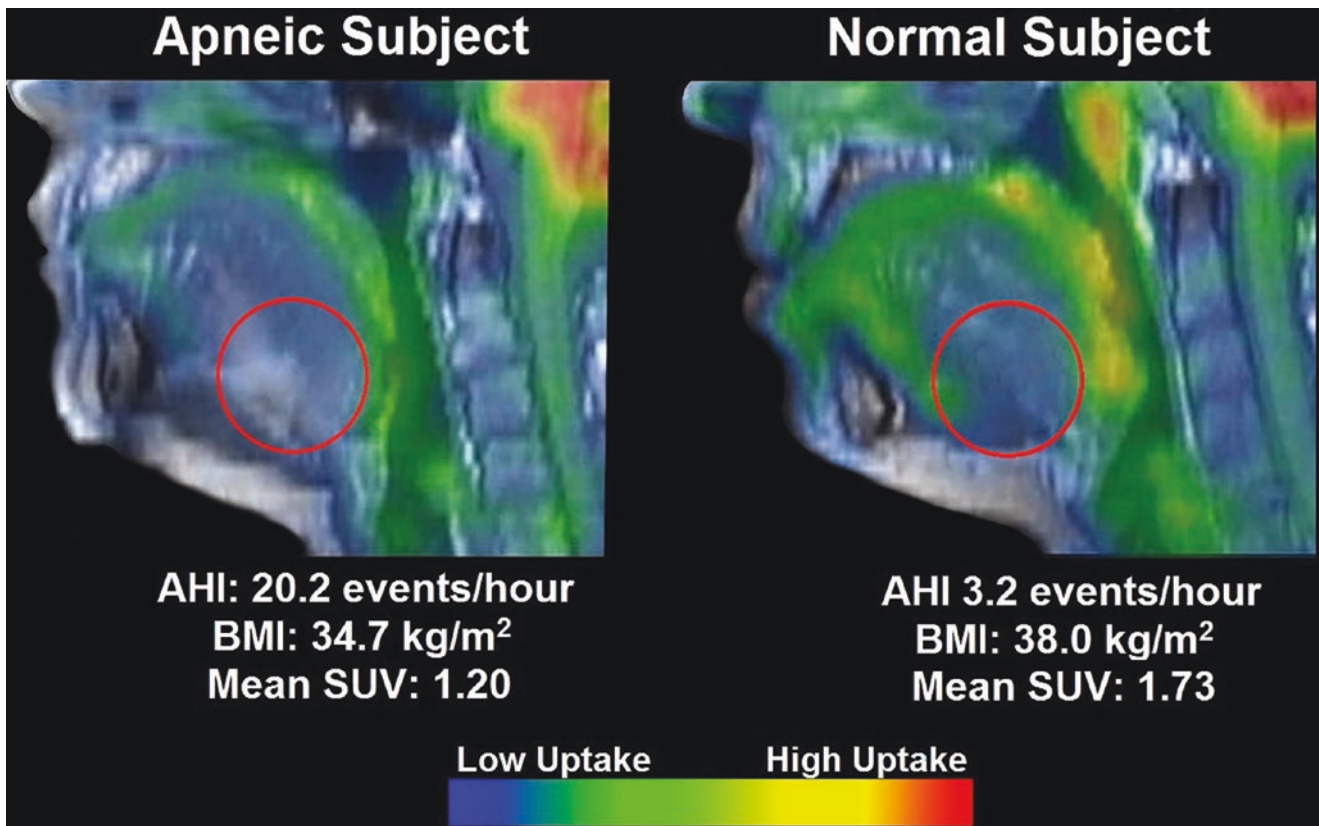


**Fig. 24** PET imaging of the tongue in an apneic and a control. Representative apneic female with reduced [18F]-2-fluoro-2-deoxy-D-glucose uptake in genioglossus in comparison with control female subject on fused positron emission tomography–magnetic resonance images. Note that the standardized uptake value (SUV) in genioglossus

of the patient with sleep apnea is reduced in comparison with the control subject. Color bars below the PET and fused MRI-PET image indicate high uptake (red) and low uptake (blue). *AHI* apnea–hypopnea index, *BMI* body mass index

## 5 Insights into the Pathogenesis of OSA with State-Dependent Upper Airway Imaging

Upper airway imaging during wakefulness has provided key insights about the risk factors and pathogenesis of sleep apnea. But the changes that occur to the upper airway during sleep (Figs. 25, 26, and 27) are fundamental to understanding the site of collapse and biomechanical changes of the pharyngeal structures during apnea or hypopnea. In a study [18] examining state-dependent changes to the upper airway in normal subjects, the volume of the retropalatal airway was reduced by 19%. The volume of the retroglottal airway

was not reduced during sleep, suggesting that the RP region may be more likely to narrow during sleep. The mean minimal cross-sectional airway area in the retropalatal region was reduced by 228% but only by 22% in the retroglottal region during sleep as compared with values during wakefulness. Reduction in the retropalatal airway area during sleep resulted from posterior movement of the soft palate, medial movement of the lateral pharyngeal walls, and posterior movement of the tongue. This study [18] used spin echo imaging over 3–4 minutes to examine state-related changes to the upper airway but newer imaging techniques [19–23] examine dynamic state-related changes to the upper airway.

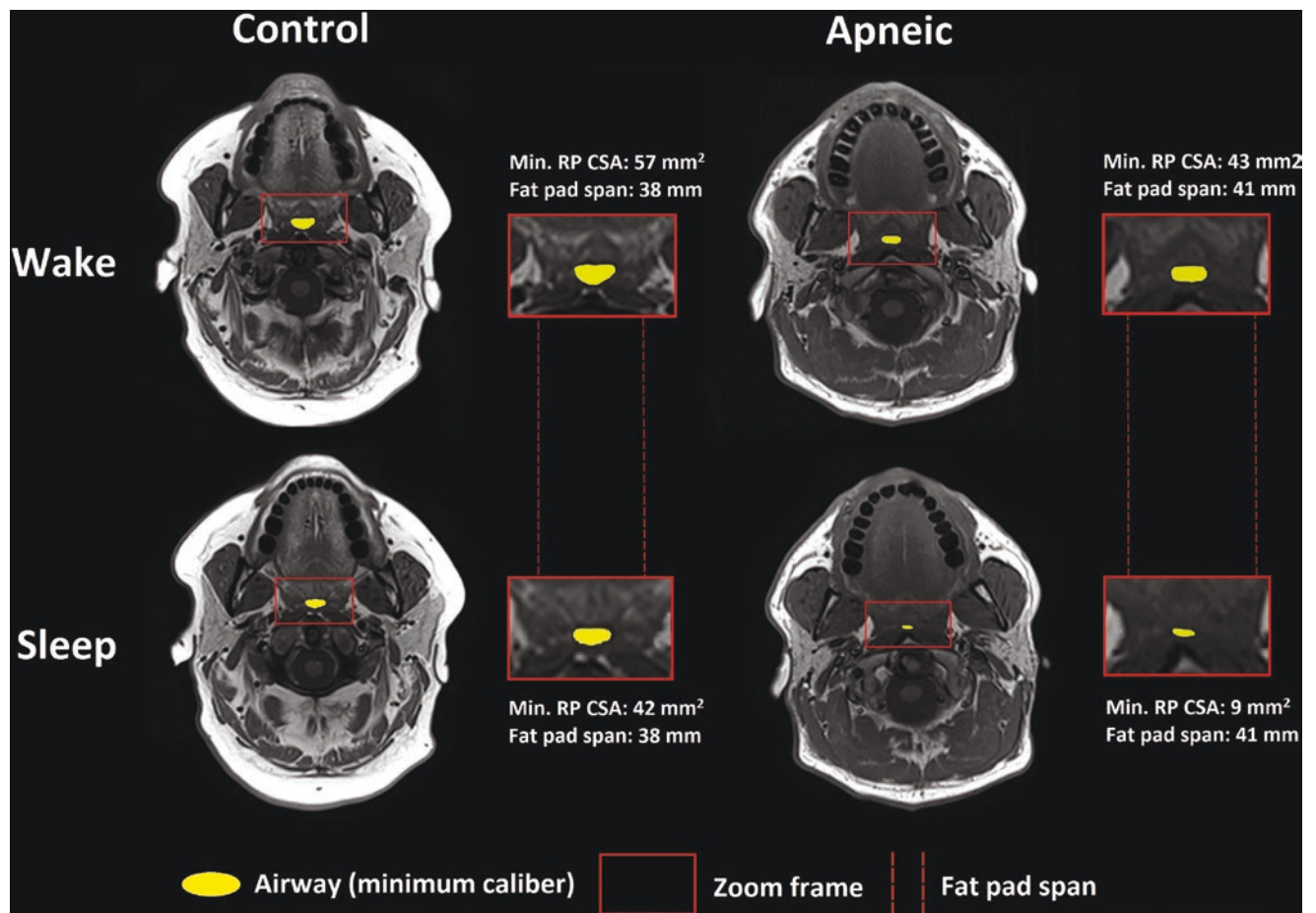


**Fig. 25** State-dependent MR imaging—changes to the airway and pharyngeal fat pads. A comparison of retropalatal axial MR images (spin echo) of control and apneic during wakefulness and sleep. Upper

airway dimensions were reduced during sleep while fat pad distance remained the same. The airway reductions with sleep were greater in the apneic than in the control. Airway is yellow

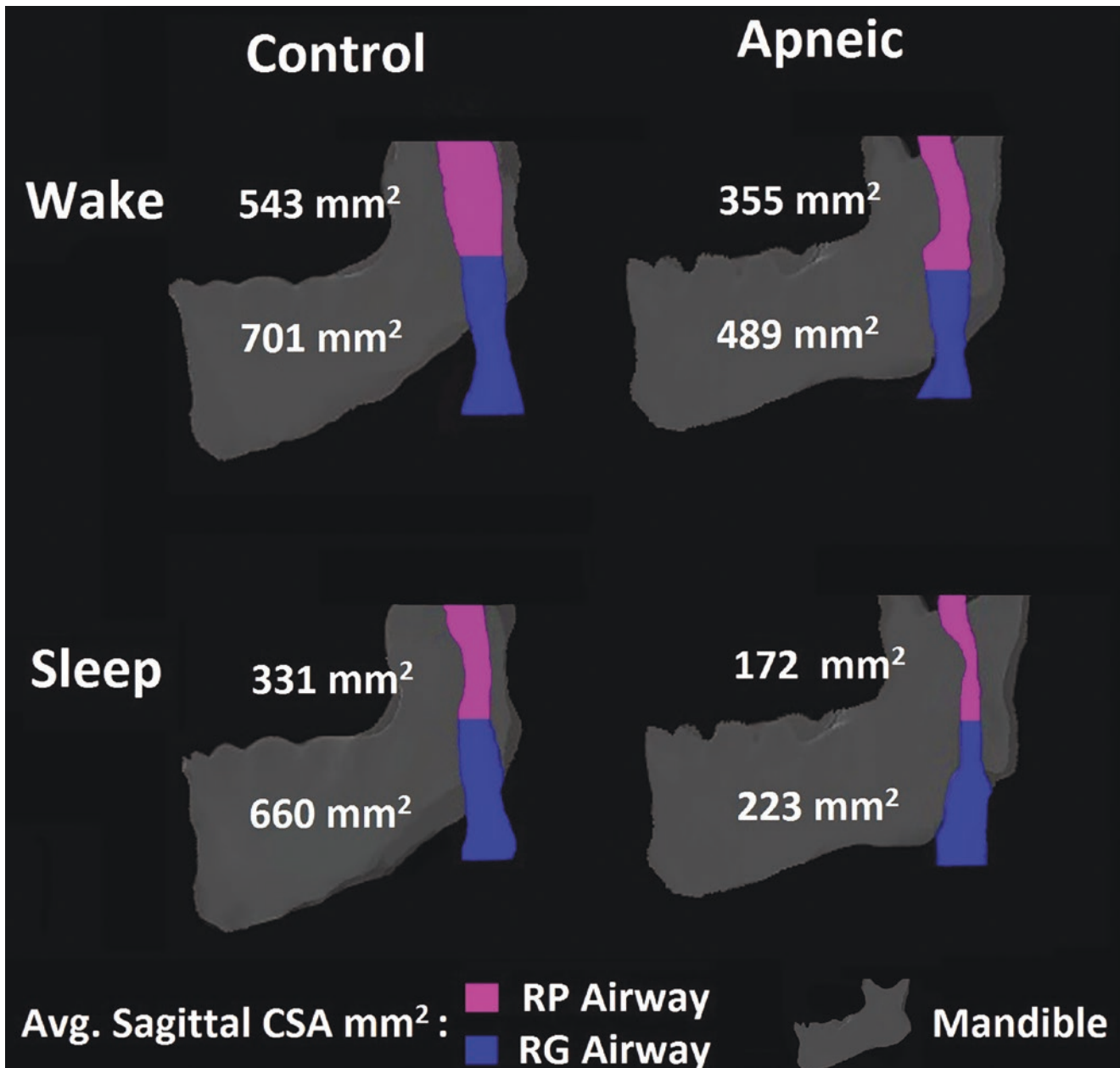


**Fig. 26** State-dependent MR imaging—changes in airway volumes. A comparison of state-dependent changes in airway volume in an apneic and a control. Narrowing during sleep is noted in the retropalatal (pink)

region in the control and apneic with narrowing in the retroglossal (blue) region in the apneic but not in the control subject

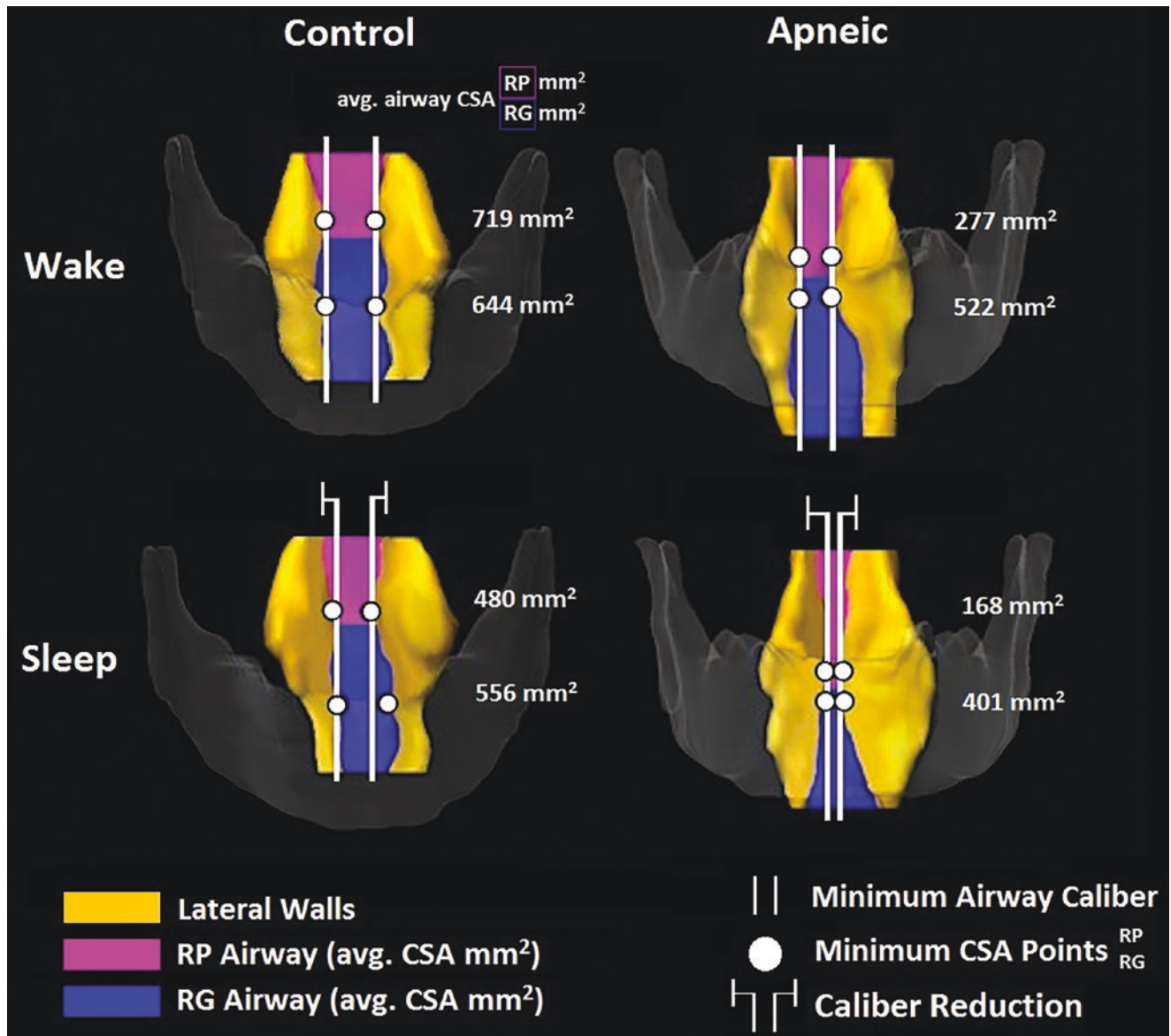


**Fig. 27** State-dependent MR imaging—changes to the airway and lateral pharyngeal walls. A comparison of state-dependent changes to the airway and lateral pharyngeal walls in an apneic and a control. The vertical lines indicate the minimal lateral airway distance in the retropalatal region during wakefulness. Note that the lateral walls move

medially during sleep. Controls show medial narrowing of the lateral pharyngeal walls in the retropalatal region while apneics show greater narrowing of the lateral pharyngeal walls in both retropalatal and retro-glossal regions

## 6 Imaging Studies Examining OSA Treatments

There are multiple effective treatments for sleep apnea including CPAP, oral appliance, weight loss, ablative upper airway surgery, and hypoglossal nerve stimulation. Upper imaging can provide insights into the mechanism of action of each of these therapeutic interventions. We will examine studies before and after these interventions in the following sections.

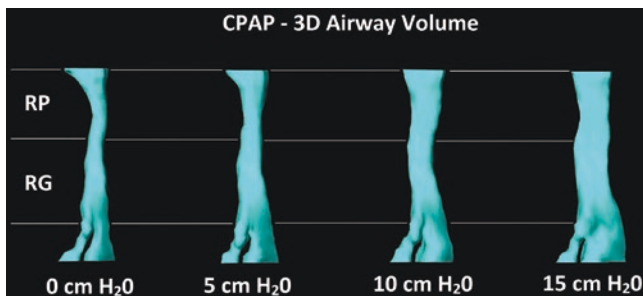
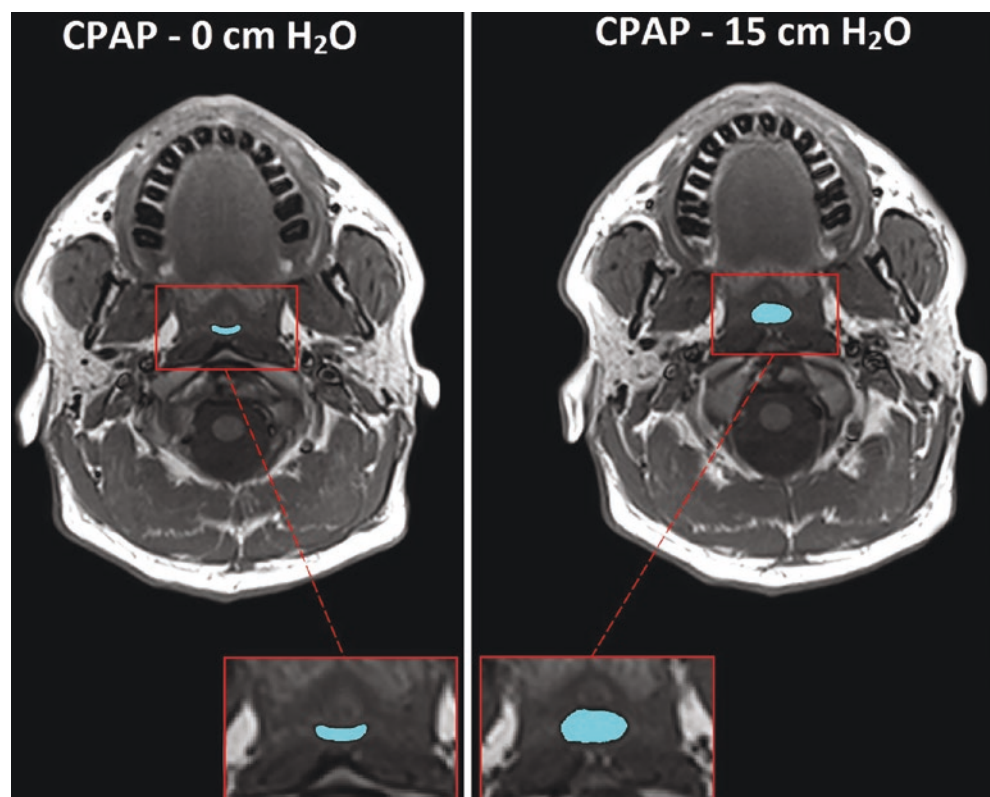


**Fig. 28** CPAP increases airway volume. Three-dimensional surface renderings of the upper airway demonstrating the effect of progressive increases in CPAP (0–15 cm of water) on upper airway volume. CPAP significantly increases airway volume in the retropalatal (RP) and retro-glossal (RG) regions in this representative subject. Note the predominant lateral airway widening with CPAP

**Fig. 29** Effect of CPAP on the upper airway. Axial MR image at the retropalatal level in a representative subject with 0 cm of water and CPAP at 15 cm of water. The increase in airway caliber with 15 cm of water is predominantly in the lateral dimension. The anterior-posterior airway dimension is relatively unchanged with CPAP at 15 cm of water



### 6.1 Imaging Studies Examining Mechanism of Action of CPAP

CPAP is the treatment of choice for patients with sleep apnea. CPAP has been shown with imaging studies [24] to increase airway caliber threefold (Figs. 28, 29, 30, and 31) in both retropalatal and retro-glossal regions. The increase in airway caliber (Figs. 28, 29, 30, and 31) is primarily in the lateral dimension secondary to reductions in the thickness of the lateral pharyngeal walls. Airway caliber (Figs. 28, 29, 30, and 31) with CPAP does not increase as much in the anterior-posterior dimension as compared to the lateral dimension.



**Fig. 30** Effect of CPAP on the lateral walls. Axial MR images at the retropalatal level in a representative subject (the same subject as in Fig. 29) with CPAP ranging from 0 to 15 cm H<sub>2</sub>O. Airway enlargement and thinning of the lateral pharyngeal wall are demonstrated with progressive increases in CPAP. The distance between the lateral pharyngeal fat pads in this subject does not appear to change with incremental increases in CPAP

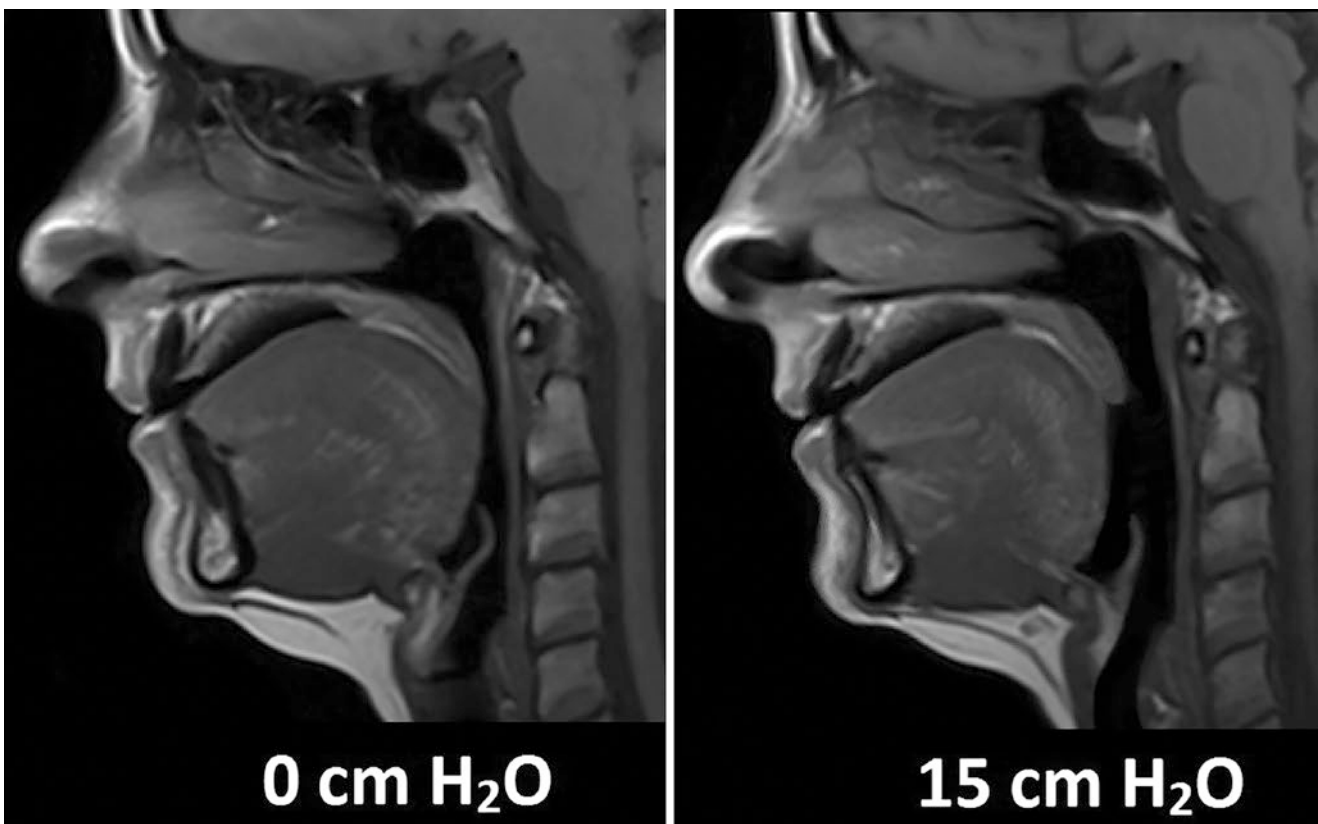


**Fig. 31** Effect of CPAP on the tongue and soft palate. Midsagittal MR image in a representative subject with 0 cm of water and CPAP at 15 cm of water. There are minimal changes in the anterior-posterior dimen-

sions of the airway with CPAP. The size and position of the tongue and soft palate also do not appear to change with CPAP at 15 cm of water

## 6.2 Imaging Studies Examining Mechanism of Action of Weight Loss

Weight loss has been shown to clinically improve sleep apnea. A study [25] using MR Dixon MR imaging (Figs. 32 and 33) has shown that weight loss decreases tongue fat and that the reduction in tongue fat is the primary mediator of the improvement in AHI (apnea–hypopnea index). Specifically, this study showed: (1) weight loss was significantly associ-

ated with reductions in tongue fat, pterygoid, and total lateral wall volumes; (2) strong correlations were observed between reductions in AHI and reductions in tongue fat volume; and (3) reduction in tongue fat volume was the primary upper airway mediator of the relationship between weight loss and AHI. These findings suggest that reductions in tongue fat may be a unique therapeutic target for patients with obesity and sleep apnea.

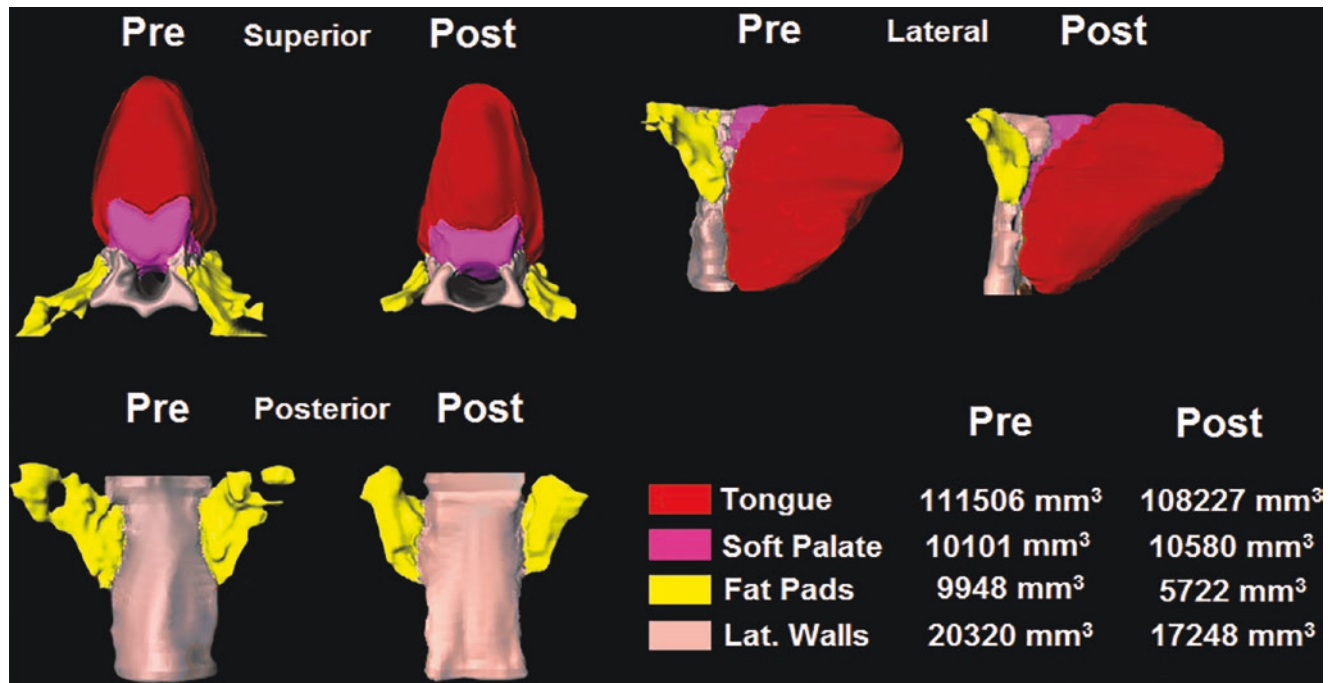


**Fig. 32** Effect of weight loss on the upper airway soft tissue structures. Three-dimensional reconstructions from axial magnetic resonance imaging (T1-weighted, spin echo, 3-mm slice thickness), demonstrating reductions in the size of upper airway soft tissue structures after 6 months of weight loss (pre to post) in a male patient with sleep apnea.

Structures include: tongue—genioglossus muscle (red); soft palate (magenta); parapharyngeal fat pads (yellow); and lateral pharyngeal walls (pink). The region extends from the superior appearance of the tongue to the appearance of the hyoid bone

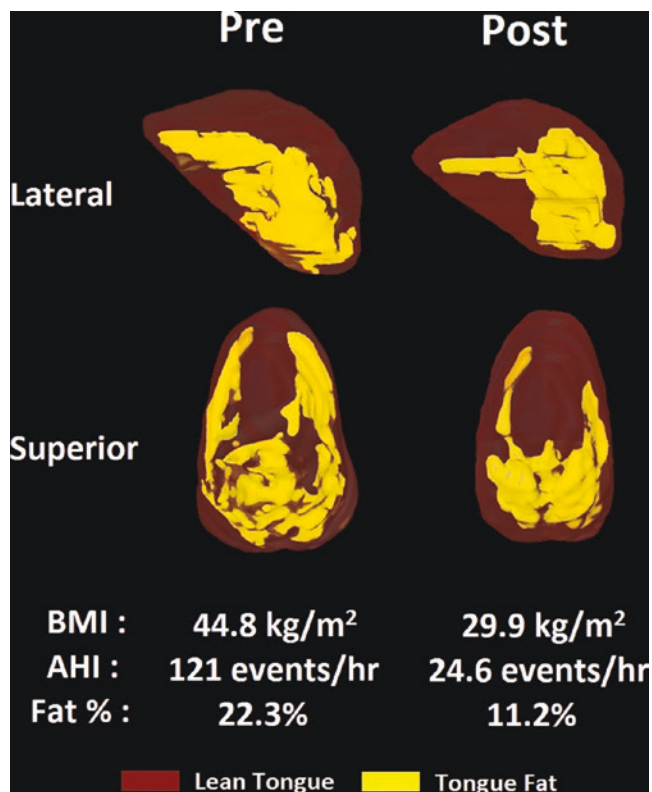


**Fig. 33** Changes in tongue fat volume with weight loss. Three-dimensional reconstructions of tongue (red/brown) and tongue fat (yellow) from axial magnetic resonance imaging (MRI; T1-weighted, spin echo, 3-mm slice thickness) and Dixon fat-only MRI (3-mm slice thickness) after 6 months of weight loss (pre to post) in a male patient with sleep apnea. These images demonstrate a significant loss of tongue fat with weight loss. Tongue fat is defined as all fat within the genioglossus muscle. *AHI* apnea–hypopnea index, *BMI* body mass index

### 6.3 Imaging Studies Examining Mechanism of Action of Oral Appliances

Oral appliances have also been shown to be an effective treatment [26, 27] for OSA. There are many different oral appliances for patients with sleep apnea and we do not know the optimal oral appliance (it may be patient dependent). Both vertical bite opening and mandibular advancement may be important in the improvement of OSA with oral appliances. Upper airway MRI (Figs. 34 and 35) can provide data on the biomechanical mechanism of action of oral appliances. In an MRI study [28], treatment with an oral appliance resulted in the following: (1) reduced the AHI from 27.0 to 12.2 events/hour; (2) increased the total airway volume predominantly because of an increase in the volume in the retropalatal region; (3) an increase in the lower anterior facial height; (4) a reduction in the distance between the hyoid and the posterior nasal spine; (5) lateral displacement of the parapharyngeal fat pads; and (6) anterior movement of the tongue base muscles. Imaging studies examining the mechanism of action of the oral appliance will be important for determining the optimal oral appliance.



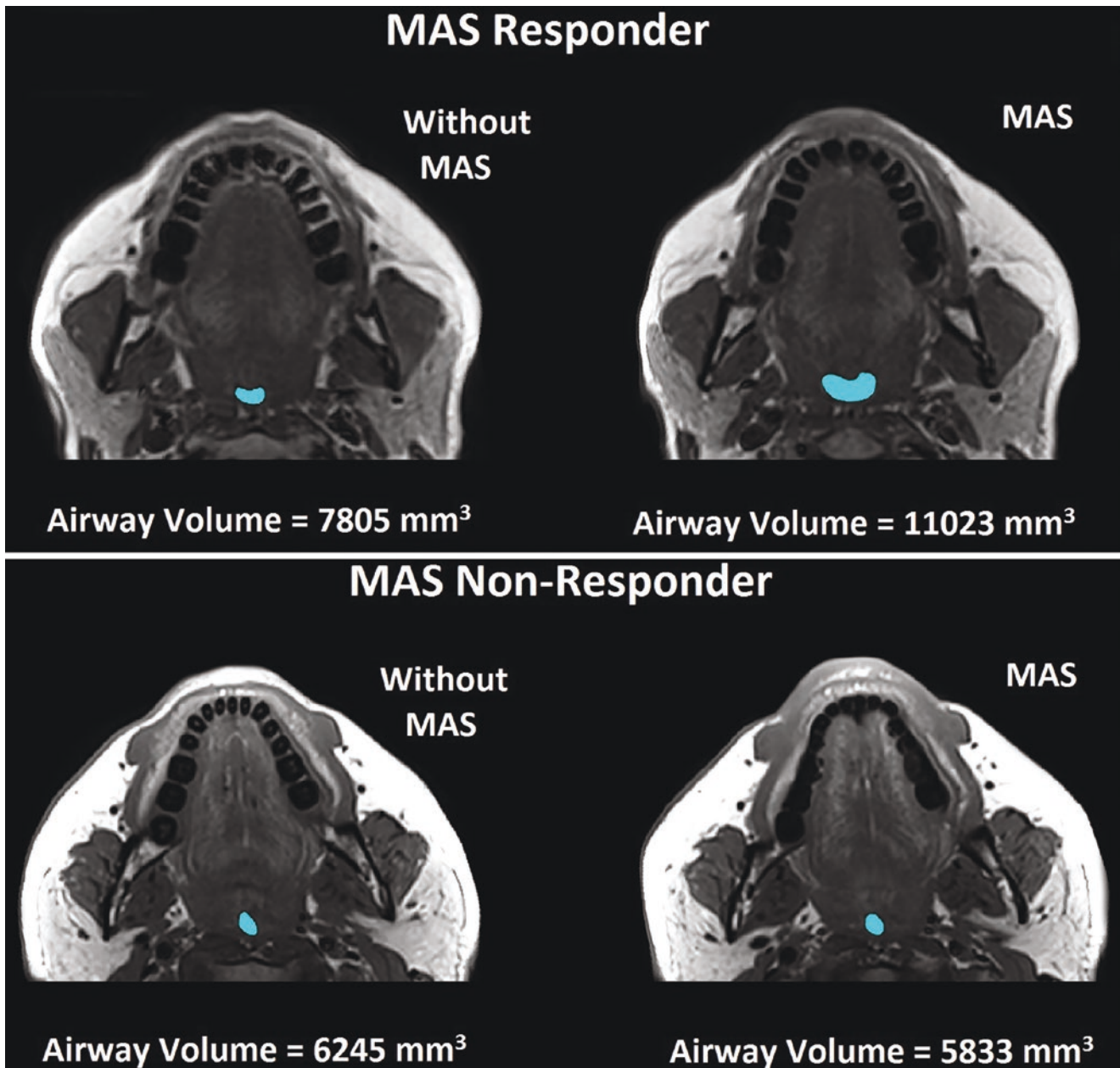


**Fig. 34** Oral appliance and the upper airway. Axial MR images from a responder and nonresponder with and without the mandibular advancement splint (MAS). In the responder, mandibular advancement increases

the caliber of the upper airway. This increase in airway size does not occur in the nonresponder

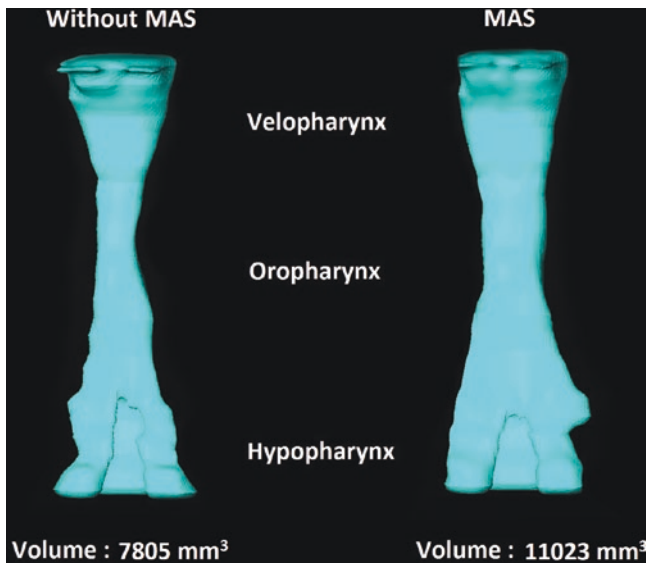


**Fig. 35** Oral appliance and volumetric changes to the upper airway. Volumetric reconstructions of the upper airway in a responder, showing an increase in the size of the upper airway with the mandibular advancement splint (MAS)

#### 6.4 Imaging Studies Examining Mechanism of Action of Ablative Upper Airway Surgery

If CPAP or oral appliances are either ineffective or not tolerated, patients may consider ablative upper airway surgery to treat their sleep apnea. The most common upper airway surgery in adults is a UPPP (uvulopalatopharyngoplasty), but other options include maxillomandibular advancement and base of tongue surgery. Transoral robotic surgery (TORS) has recently become a new surgical approach [29–31] for the treatment of OSA because it allows for better access to the base of the tongue compared to conventional procedures. Volumetric MRI [32] can be an important tool (Figs. 36 and 37) to understand the postsurgical anatomic changes and reasons for success/nonsuccess in all sleep surgeries (including TORS). Accordingly, upper airway MRIs [32] were performed pre- and postoperatively in apneics undergoing TORS (surgery included bilateral posterior hemiglossectomy with limited pharyngectomy and uvulopalatopharyngoplasty). Pre- to postoperative changes from this study [32] included: (1) a 19.4% increase in total airway volume; (2) decreases in the soft palate and tongue volumes by 18.3% and 5.8%, respectively; (3) decreases in retropalatal and total lateral wall volumes by 49.8% and 17.9%, respectively; (4) no volumetric changes in other structures; and (5) reductions in retropalatal lateral wall volume correlated with decreased AHI. Such studies indicate that volumetric MRI is an important tool to understand the postsurgical anatomic changes and reasons for success in all types of sleep surgery (including TORS).

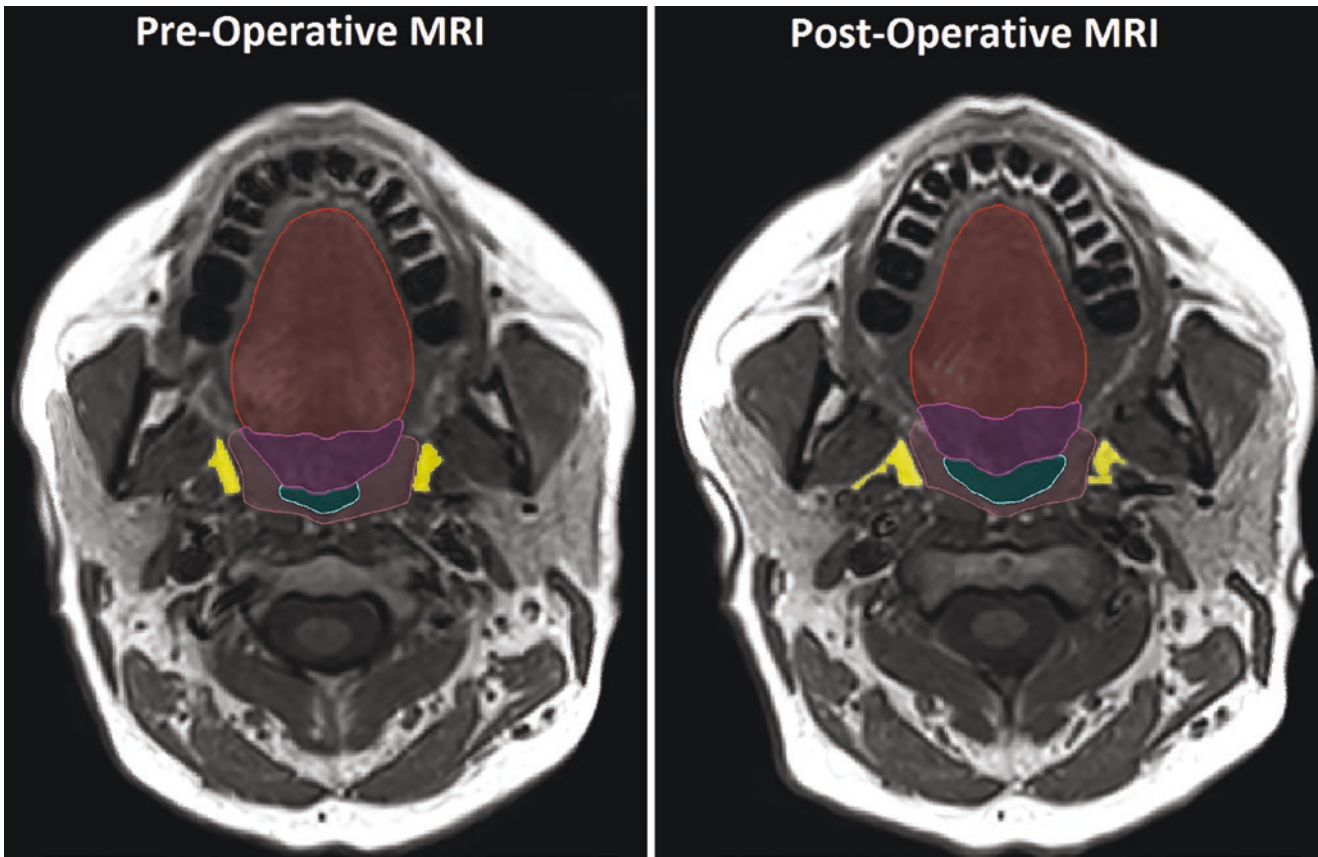


**Fig. 36** Upper airway MRI before and after pharyngeal surgery. Magnetic resonance imaging segmentation shown in a patient pre- and postoperatively after upper airway surgery at comparable cross-sectional regions showing an increase in airway volume at the retro-

palatal airway level. Color key: light blue = retropalatal airway; purple = soft palate; red = genioglossus tongue; brown = retropalatal lateral/posterior walls; yellow = parapharyngeal fat pads

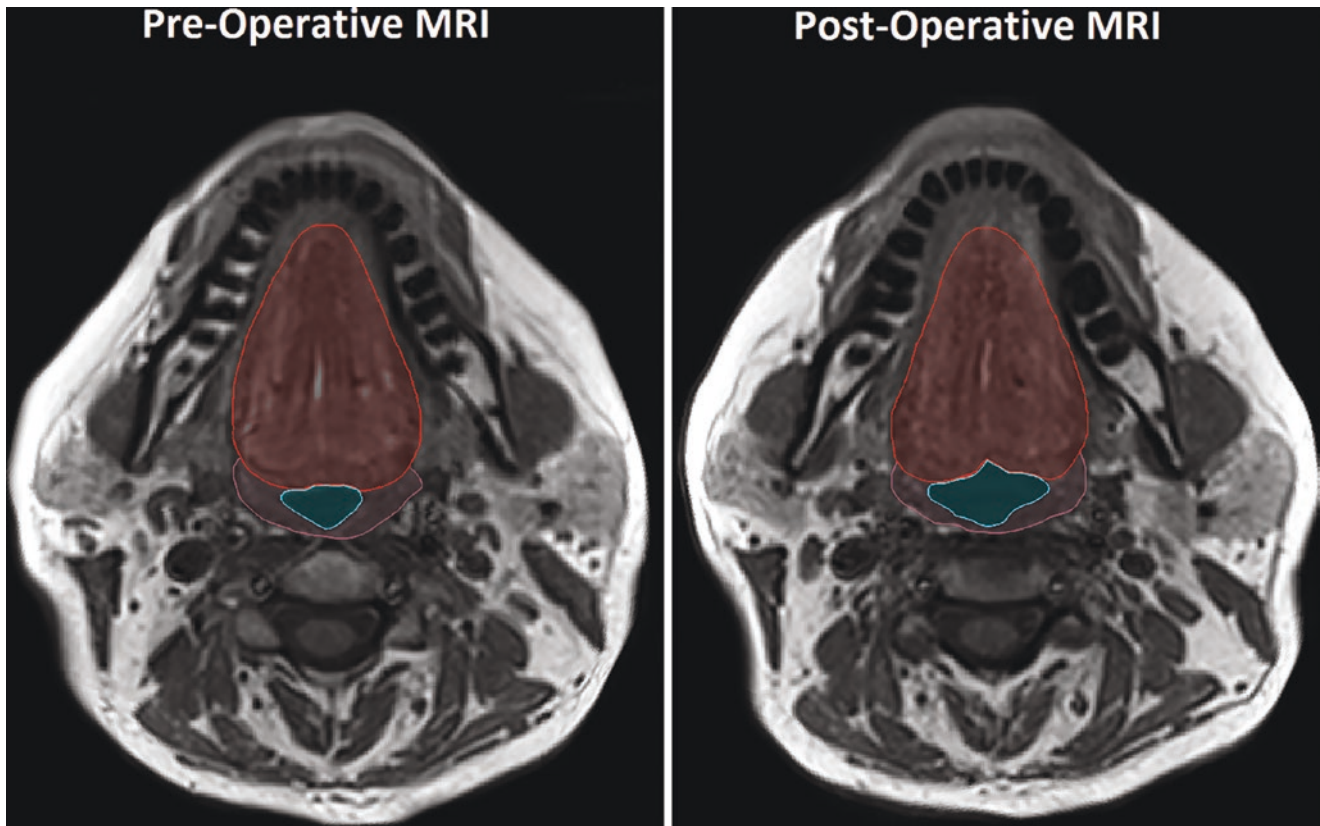


**Fig. 37** Upper airway MRI before and after pharyngeal surgery. Magnetic resonance imaging segmentation shown in a patient pre- and postoperatively after upper airway surgery at comparable cross-

sectional regions showing an increase in airway volume at the retroglossal airway level. Color key: light blue = retroglossal airway; red = genioglossus tongue; brown = retropalatal lateral/posterior walls

## 6.5 Imaging Studies Examining Mechanism of Action of Hypoglossal Nerve Stimulation

Recently hypoglossal nerve stimulation has been utilized for OSA treatment [33]. This surgery has a distinct advantage over other surgeries for sleep apnea since it is reversible and effective. We can understand the mechanism of action of hypoglossal nerve stimulation (Figs. 38, 39, and 40) with CT scanning [34]. A CT imaging study [34] with hypoglossal nerve stimulation during wakefulness was used to examine differences in upper airway caliber, the volume of the upper

airway soft tissue structures, craniofacial relationships, and centroid tongue and soft palate position in responders and nonresponders. These data indicated responders had a smaller baseline soft palate volume compared to nonresponders. During stimulation, responders compared to nonresponders had: (1) a larger increase in the retroglossal airway size; (2) greater shortening of the mandible-hyoid distance (hyoid movement toward the mandible); and (3) increased anterior displacement of the tongue (based on the tongue centroids). Such data indicate that we can understand the mechanism of action of hypoglossal nerve stimulation with CT scanning.

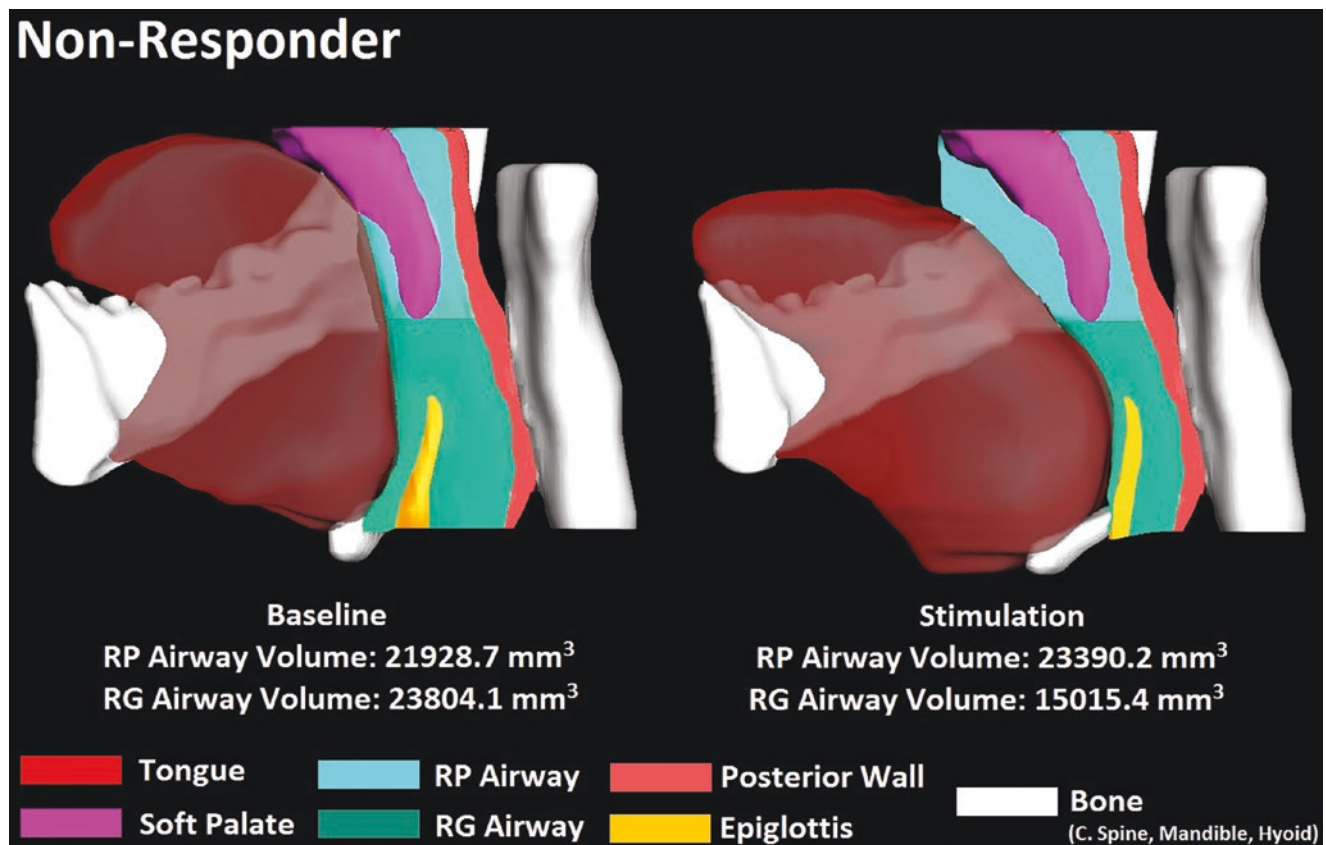


**Fig. 38** Upper airway CT in a nonresponder undergoing hypoglossal nerve stimulation. Midsagittal reconstruction with computed tomography imaging during wakefulness in a nonresponder before and during hypoglossal nerve stimulation. The stimulation caused tongue tip protrusion and inferior displacement and also resulted in tongue base retru-

sion causing narrowing of the retroglossal airway. Color key: teal = retropalatal airway; green = retroglossal airway; red = genioglossus tongue; pink = soft palate; orange = posterior wall; yellow = epiglottis; white = bone (C {cervical} spine, mandible, hyoid)

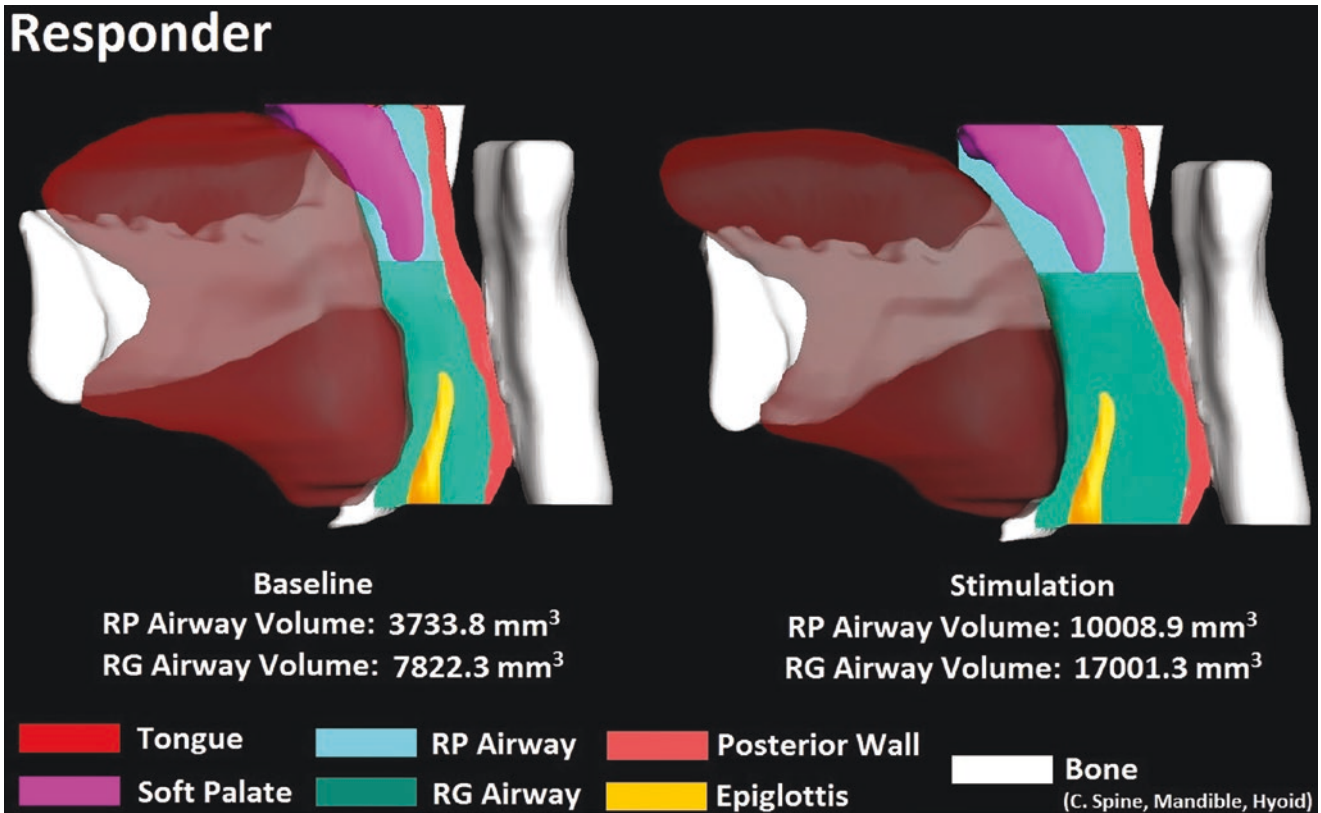


**Fig. 39** Upper airway CT in a responder undergoing hypoglossal nerve stimulation. Midsagittal reconstruction with computed tomography imaging during wakefulness in a responder before and during hypoglossal nerve stimulation. The stimulation caused the anterior and inferior displacement of the tongue and hyoid bone with a resultant

increase in the RP and RG airway. Color key: teal = retropalatal airway; green = retroglottal airway; red = genioglossus tongue; pink = soft palate; orange = posterior wall; yellow = epiglottis; white = bone (C {cervical} spine, mandible, hyoid)

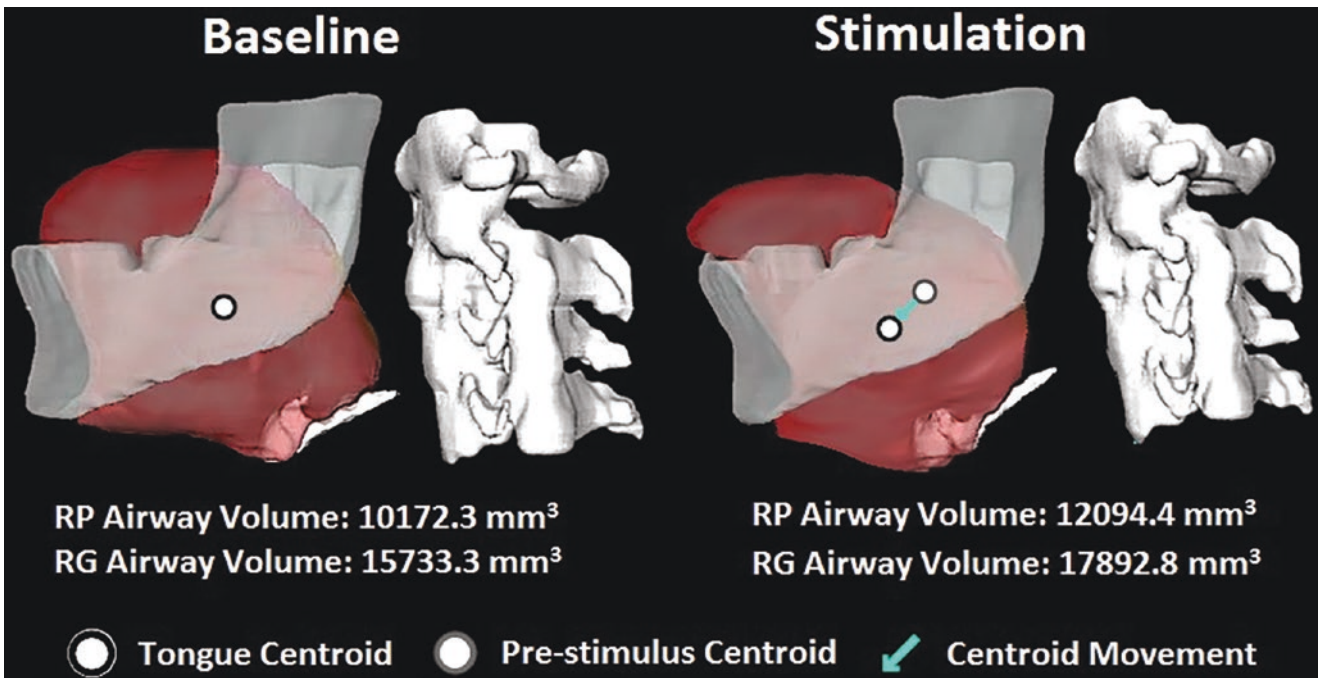


**Fig. 40** Effects of hypoglossal nerve stimulation on the tongue centroid and airway volume. 3D reconstruction with computed tomography imaging during wakefulness in a responder showing the location of the tongue centroid at baseline and with hypoglossal nerve stimulation.

The tongue centroid shifted anteriorly and inferiorly (teal arrow) with stimulation, with an increase in the retropalatal and retroglottal airway volumes

## References

1. Neelapu BC, Kharbanda OP, Sardana HK, Balachandran R, Sardana V, Kapoor P, et al. Craniofacial and upper airway morphology in adult obstructive sleep apnea patients: A systematic review and meta-analysis of cephalometric studies. *Sleep Med Rev.* 2017;31(1532–2955 (Electronic)):79–90.
2. Agha B, Johal A. Facial phenotype in obstructive sleep apnea-hypopnea syndrome: a systematic review and meta-analysis. *J Sleep Res.* 2017;26(2):122–31.
3. Chen H, Aarab G, de Ruiter MHT, de Lange J, Lobbezoo F, van der Stelt PF. Three-dimensional imaging of the upper airway anatomy in obstructive sleep apnea: a systematic review. *Sleep Med.* 2016;21:19–27.
4. Schwab R, Pasirstein M, Pierson R, Mackley A, Hachadoorian R, Arens R, et al. Identification of upper airway anatomic risk factors for obstructive sleep apnea with volumetric magnetic resonance imaging. *Am J Respir Crit Care Med.* 2003;168(5):522–30.
5. Kim AM, Keenan BT, Jackson N, Chan EL, Staley B, Poptani H, et al. Tongue fat and its relationship to obstructive sleep apnea. *Sleep.* 2014;37(10):1639–48.
6. Chi L, Comyn FL, Mitra N, Reilly MP, Wan F, Maislin G, et al. Identification of craniofacial risk factors for obstructive sleep apnoea using three-dimensional MRI. *Eur Respir J.* 2011;38(2):348–58.
7. Lahav Y, Rosenzweig E, Heyman Z, Doljansky J, Green A, Dagan Y. Tongue base ultrasound: a diagnostic tool for predicting obstructive sleep apnea. *Ann Otol Rhinol Laryngol.* 2009;118(3):179–84.
8. Shu CC, Lee P, Lin JW, Huang CT, Chang YC, Wang HC. The use of sub-mental ultrasonography for identifying patients with severe obstructive sleep apnea. *PLoS One.* 2013;8(5):e62848.
9. Liao LJ, Cho TY, Cheng PW, Wang CT, Lo WC, et al. Submental ultrasonography in diagnosing severe obstructive sleep apnea syndrome. *J Med Ultrasound.* 2016;24(3):107–11.
10. Bilici S, Engin A, Ozguz Y, Onerci CO, Gorkem YA, Hande YA. Submental ultrasonographic parameters among patients with obstructive sleep apnea. *Otolaryngol Head Neck Surg.* 2017;156(3):559–66.
11. Yu JL, Wiemken A, Schultz SM, Keenan BT, Sehgal CM, Schwab RJ. A comparison of ultrasound echo intensity to magnetic resonance imaging as a metric for tongue fat evaluation. *Sleep.* 2022;45(2):zsab295.
12. Feng Y, Keenan BT, Wang S, Leinwand S, Wiemken A, Pack AI, et al. Dynamic upper airway in obese apneics and obese controls. *Am J Respir Crit Care Med.* 2018;198(11):1435–43.
13. Kezirian EJ, Hohenhorst W, De Vries N. Drug-induced sleep endoscopy: the VOTE classification. *Eur Arch Otorhinolaryngol.* 2011;268(8):1233–6.
14. Borek R, Schwab RJ, Thaler E, Kim C, Jackson N, Mandel JE. Quantitative airway analysis during drug-induced sleep endoscopy for evaluation of sleep apnea. *Laryngoscope.* 2012;122(11):2592–9.
15. Kim AM, Keenan BT, Jackson N, Chan EL, Staley B, Torigian DA, et al. Metabolic activity of the tongue in obstructive sleep apnea: a novel application of FDG positron emission topography imaging. *Am J Respir Crit Care Med.* 2014;189(11):1416–25.
16. Cohen O, John MM, Kaufman AE, Kundel V, Burschtin O, Khan S, et al. Novel non-invasive assessment of upper airway inflammation in obstructive sleep apnea using positron emission tomography/magnetic resonance imaging. *Sleep Breath.* 2022;26(3):1087–96.
17. Cohen O, Kaufman AE, Choi H, Khan S, Robson PM, Suárez-Fariñas M, et al. Pharyngeal inflammation on positron emission tomography/magnetic resonance imaging before and after obstructive sleep apnea treatment. *Ann Am Thorac Soc.* 2023;20(4):574–83. Dec 7; Epub ahead of print
18. Trudo FJ, Geftter WB, Welch KC, Gupta KB, Maislin G, Schwab RJ. State-related changes in upper airway caliber and surrounding soft-tissue structures in normal subjects. *Am J Respir Crit Care Med.* 1998;158(4):1259–70.
19. Nayak KS, Fleck RJ. Seeing sleep: dynamic imaging of upper airway collapse and collapsibility in children. *IEEE Pulse.* 2014;5(5):40–4.
20. Moon IJ, Han DH, Kim JW, Rhee CS, Sung MW, Park JW, et al. Sleep magnetic resonance imaging as a new diagnostic method in obstructive sleep apnea syndrome. *Laryngoscope.* 2010;120(12):2546–54.
21. Donnelly LF, Surdulescu V, Chini BA, Casper KA, Poe SA, Amin RS. Upper airway motion depicted at cine MR imaging performed during sleep: comparison between young patients with and those without obstructive sleep apnea. *Radiology.* 2003;227(1):239–45.
22. Darquenne C, Elliott AR, Sibille B, Smales ET, DeYoung PN, Theilmann RJ, et al. Upper airway dynamic imaging during tidal breathing in awake and asleep subjects with obstructive sleep apnea and healthy controls. *Physiol Rep.* 2018;6(10):e13711.
23. Kim YC. Fast upper airway magnetic resonance imaging for assessment of speech production and sleep apnea. *Precis Fut Med.* 2018;2(4):131–48.
24. Schwab RJ, Pack AI, Gupta KB, Metzger LJ, Oh E, Getsy JE, et al. Upper airway and soft tissue structural changes induced by CPAP in normal subjects. *Am J Respir Crit Care Med.* 1996;154(4 Pt 1):1106–16.
25. Wang SH, Keenan BT, Wiemken A, Zang Y, Staley B, Sarwer DB, et al. Effect of weight loss on upper airway anatomy and the apnea-hypopnea index. The importance of tongue fat. *Am J Respir Crit Care Med.* 2020;201(6):718–27.
26. Sutherland K, Cistulli PA. Oral appliance therapy for obstructive sleep apnoea: state of the art. *J Clin Med.* 2019;8(12):2121.
27. Phillips CL, Grunstein RR, Darendeliler MA, Mihailidou AS, Srinivasan VK, Yee BJ, et al. Health outcomes of continuous positive airway pressure versus oral appliance treatment for obstructive sleep apnea: a randomized controlled trial. *Am J Respir Crit Care Med.* 2013;187(8):879–87.
28. Chan ASL, Sutherland K, Schwab RJ, Zeng B, Petocz P, Lee RWW, Darendeliler M, Cistulli PA. The effect of mandibular advancement on upper airway structure in obstructive sleep apnoea. *Thorax.* 2010;65(8):726–32.
29. Vicini C, Dallan I, Canzi P, Frassinetti S, Nacci A, Seccia V, et al. Transoral robotic surgery of the tongue base in obstructive sleep apnea-hypopnea syndrome: anatomic considerations and clinical experience. *Head Neck.* 2012;34(1):15–22.
30. Friedman M, Hamilton C, Samuelson CG, Kelley K, Taylor D, Pearson-Chauhan K, et al. Transoral robotic glossectomy for the treatment of obstructive sleep apnea-hypopnea syndrome. *Otolaryngol Head Neck Surg.* 2012;146(5):854–62.
31. Lin HS, Rowley JA, Badr MS, Folbe AJ, Yoo GH, Victor L, et al. Transoral robotic surgery for treatment of obstructive sleep apnea-hypopnea syndrome. *Laryngoscope.* 2013;123(7):1811–6.
32. Chiffer RC, Schwab RJ, Keenan BT, Borek RC, Thaler ER. Volumetric MRI analysis pre- and post-transoral robotic surgery for obstructive sleep apnea. *Laryngoscope.* 2015;125(8):1988–95.
33. Strollo PJ Jr, Soose RJ, Maurer JT, de Vries N, Cornelius J, Froyovich O, for the STAR Trial Group, et al. Upper-airway stimulation for obstructive sleep apnea. *N Engl J Med.* 2014;370(2):139–49.
34. Schwab RJ, Wang SH, Verbraecken J, Vanderveken OM, Van de Heyning P, Vos WG, et al. Anatomic predictors of response and mechanism of action of upper airway stimulation therapy in patients with obstructive sleep apnea. *Sleep.* 2018;41(4):zsy021.